Progress in Polymer Science 134 (2022) 101608

Contents lists available at ScienceDirect

Progress in Polymer Science

journal homepage: www.elsevier.com/locate/progpolymsci

Synthetic biodegradable polyhydroxyalkanoates (PHAs): Recent advances and future challenges

Andrea H. Westlie, Ethan C. Quinn, Celine R. Parker, Eugene Y.-X. Chen*

Department of Chemistry, Colorado State University, Fort Collins, CO 80523-1872, USA

ARTICLE INFO

Article history:
Received 14 July 2022
Revised 9 September 2022
Accepted 14 September 2022
Available online 15 September 2022

ABSTRACT

This article reviews the advances made over the past five decades of research in developing effective chemocatalytic pathways to synthesize polyhydroxyalkanoates (PHAs), a prominent class of biodegradable polyesters found in nature and considered as sustainable alternatives to petroleum-based non-degradable plastics. Focused in this review are recent efforts that seek to address the key challenges facing the biosynthetic routes by taking advantage of precision in synthesis, expedient tunability in polymer stereomicrostructures and structures of monomers and molecular catalysts, as well as scalability and speed in polymer production that chemical catalysis can offer. This article is organized by poly(3-hydroxybutyrate) (P3HB) stereomicrostructures (tacticities), from isotactic to syndiotactic to atactic P3HB materials, followed by other PHA homopolymers and copolymers. Under each type of stereochemically defined PHAs, monomers, catalysts, and polymerizations employed for the synthesis, as well as mechanistic aspects when possible, are described. Next, recent advances in expanding the PHA scope and developing functionalized, uncommon or unnatural PHAs, inaccessible by biological methods, especially block and stereoblock or stereosequenced PHAs, are highlighted in their synthetic methods and advanced materials properties. Lastly, four key remaining challenges, and thus corresponding future directions directed at addressing those challenges, are discussed.

List of abbreviations

Ad	adamantyl
at-	atactic
BCP	block copolymer
BDI	β-diiminate
BEMP	2-*tert*-butylimino-2-diethylamino-1,3-dimethylperhydro-1,3,2-diazaphosphorine
BINAP	([1,1′-binaphthalene]-2,2′-diyl)bis(diphenylphosphane)
BPL^{OR}	β-propiolactone
CHO	cyclohexene oxide
ClTPP	*meso*-tetra(4-chlorophenyl)porphyrinato
cumyl	-Me_2Ph
$Đ$	dispersity
DBU	1,8-diazabicyclo[5.4.0]-undec-7-ene
$dMMLA^{Bz}$	dimethyl benzyl β-malolactone
DSC	differential scanning calorimetry
E	young's modulus
e.e.	enantiomeric excess
$8DL^{Me}$	8-membered dimethyl diolide (cyclic dimer of 3-hydroxybutyric acid)
EoL	end-of-life
EtioP	etioporphyrin
HDPE	high-density polyethylene
IBAO	isobutylaluminoxane
IMes	1,3-bis(2,4,6-trimethylphenyl)imidazole-2-ylidene
it-	isotactic
LDPE	low-density polyethylene
MAO	methylaluminoxane
mcl-	medium-chain length
meso-	a non-optically active member of a set of stereoisomers
MLA^{Bz}	benzyl-β-malolactone
M_n	number-average molecular weight
NHC	*N*-heterocyclic carbene
NMR	nuclear magnetic resonance
Nu	nucleophile
n.r.	not reported
P3HB	poly(3-hydroxybutyrate)
P3HBHp	poly(3-hydroxybutyrate-*co*-hydroxyheptanoate)
P3HBV	poly(3-hydroxybutyrate-*co*-hydroxyvalerate)
P3HD	poly(3-hydroxydecanoate)
P3HDD	poly(3-hydroxydodecanoate)
P3HHp	poly(3-hydroxyheptanoate)
P3HHx	poly(3-hydroxyhexanoate)

* Corresponding author.
E-mail address: eugene.chen@colostate.edu (E.Y.-X. Chen).

https://doi.org/10.1016/j.progpolymsci.2022.101608
0079-6700/

P3HO	poly(3-hydroxyoctanoate)
P3H4PhB	poly(3-hydroxy-4-phenylbutyrate)
P3HV	poly(3-hydroxyvalerate)
P4HB	poly(4-hydroxybutyrate) or poly(γ-butyrolactone)
PBAT	poly(butylene adipate terephthalate)
PBPL^{OR}	poly(β-propiolactone)
PBS	poly(butylene succinate)
PCHC	poly(cyclohexene carbonate)
PCL	poly(ε-caprolactone)
PDL	poly(ε-decalactone)
PdMMLA	poly([*R/S*]-3,3-dimethylmalic acid)
PHA	polyhydroxyalkanoate
P_m	probability of *meso* linkages between two consecutive monomer units
PMLA^{Bz}	poly(benzyl-β-malolactone)
PPN	bis(triphenylphosphine)iminium
P_r	probability of *rac* linkages between two consecutive monomer units
PP	polypropylene
rac-	*racemic,* an equal mixture of left-handed and right-handed enantiomers in a solution
ROP	ring-opening polymerization
sb-	stereoblock
scl	short-chain length
st-	syndiotactic
TBD	1,5,7-triazabicyclo[4.4.0]dec-5-ene
T_c	crystallization temperature
T_d	degradation temperature
T_g	glass-transition temperature
T_m	melting-transition temperature
TMS	trimethylsilane
TPPAlCl	(tetraphenylporphinato)(TPP)aluminum chloride
TPT	1,3,4-triphenyl-4,5-dihydro-*1H*-1,2,4-triazol-5-ylidene
β-BL	β-butyrolactone
β-VL	β-valerolactone
γ-BL	γ-butyrolactone
ΔH	enthalpy of fusion
ε-CL	ε-caprolactone
ε_B	elongation at break
σ	ultimate tensile strength

1. Introduction

Polyhydroxyalkanoates (PHAs) are biologically produced, biocompatible polyesters that are ubiquitous in Nature and living systems, and they have thus gained increasing attraction as biodegradable plastic alternatives for a variety of applications that emphasize better end-of-life (EoL) options and environmental protection [1–7]. PHAs have been shown to be biodegradable under ambient conditions in both managed and unmanaged environments [8–11]. The most commonly produced PHA in the large PHA family that includes more than 150 known structures—which are defined as, and limited to, poly(3-hydroxyacid)s in this review, poly(3-hydroxybutyrate) (P3HB), exhibits several desirable materials characteristics including its high crystallinity, perfect isotacticity with each pendant group having exclusively (*R*)-configuration, high melting-transition temperature (T_m) up to ~180 °C, good ultimate tensile strength (σ = ~40 MPa), and excellent barrier to oxygen and moisture transport [12,13]. Despite those attractive performance properties, P3HB suffers from low thermostability towards melt-processing, with a degradation temperature (T_d, defined as the temperature at 5% weight loss) around 250 °C, and brittleness, with an extremely low elongation at break (ε_B ~3-6%), therefore largely limiting its wider industrial applications as a commodity plastic.

The development of fermentation routes from biorenewable feedstocks to P3HB and copolymers of P3HB with short-chain length (*scl*, C_4–C_5) and medium-chain length (*mcl*, C_6–C_{14}) comonomers has resulted in the commercial utilities of PHAs (A, Fig. 1). There are several reviews highlighting the developments and advancements of biological routes towards PHAs [14–26]. However, the high cost of the current biological production of PHAs represents a major bottleneck in their large-scale commercialization [27]. In addition, biological routes are limited by the step-growth polymerization mechanism where incorporation of 3-hydroxybutyrate is most common, thus engineering of the metabolic pathways is typically required for tuning of PHA compositions [3,28]. For example, bacteria synthesize different PHAs from coenzyme-A thioesters of hydroxyalkanoic acids via polycondensation, which produce PHAs with a high dispersity ($Đ$) ≥ 2.0, thus not suitable for synthesizing well-defined block copolymers (BCPs). There is evidence that periodic feeding of microorganisms can result in some "blocky" PHA copolymers that can be fractionated out of the whole polymer product [29,30]. Although the thermal and mechanical properties of these fractionated blocky copolymers were different than the homo- and random copolymers, the evidence overall is lacking for the formation of well-defined BCPs. Furthermore, despite the tunability of the chiral repeat units of the backbone, which allows for generation of various stereomicrostructures (tacticities) including isotactic (*it*), syndiotactic (*st*), atactic (*at*), and stereoblock (*sb*) microstructures (Fig. 1), biologically derived PHAs are exclusively accumulated as *it*-polymers with absolute (*R*)-stereoconfiguration.

Like other classes of polymers, thermal and mechanical properties of polyesters can generally be tuned by manipulating the polymer stereomicrostructure [31–34], topology [35], and pendant group structure [36]. In this context, several advantages of chemocatalytic routes towards PHAs can be envisioned, in principle, including: (i) *precision in synthesis* (control of chain length (M_n) and $Đ$, comonomer sequence, and architecture); (ii) *tunability* in polymer stereomicrostructure (*it, st, at, sb*-tacticities and *R* or *S* stereoconfigurations), molecular catalyst structure (symmetry and chirality, thus, stereoselectivity), and co/polymer structure (limitless designed monomers); and (iii) *scalability and speed* in production (ease in processing and fast reaction kinetics typically associated with catalyzed ring-opening polymerization (ROP) processes). However, currently a major challenge for the chemocatalytic route to PHAs is the need to develop cost-effective synthesis of monomers (from renewable feedstocks) and catalysts and ideally establish "monomer-polymer-monomer" closed-loop lifecycles of PHAs, in addition to their biodegradation EoL option. The key differentiating and overlapping features of both biological and chemical synthetic routes towards PHAs are highlighted in Fig. 2.

Four key chemocatalytic routes towards PHAs, represented by P3HB herein, are summarized in Fig. 1. The direct route is polycondensation of (*R*)-3-hydroxybutyric acid, which affords *it*-P[(*R*)-3HB] (B, Fig. 1). However, this method is prone to crotonization, the formation of crotonate end groups through transesterification side reactions or elimination/termination reactions (Scheme 2); hence, polycondensation is not a suitable route towards high-molecular-weight P3HB [2,37–39]. On the other hand, the ROP, which proceeds via a chain-growth mechanism with fast initiation and propagation kinetics, can produce P3HB with high molecular weights, low $Đ$ values, and tunable tacticities. In this context, the ROP of the 4-membered β-butyrolactone (β-BL) leads to P3HB with various tacticities, depending on the stereoselectivity of the catalyst (C, Fig. 1). The direct carbonylative polymerization of propylene oxide and CO results in the formation of atactic P3HB (D, Fig. 1). In comparison, the ROP of the 8-membered cyclic dimer of 3-hydroxybutyric acid, 8DL^{Me} (E, Fig. 1), which bears two chiral centers and thus exists in three diastereomeric forms (*R,R/S,S racemic*

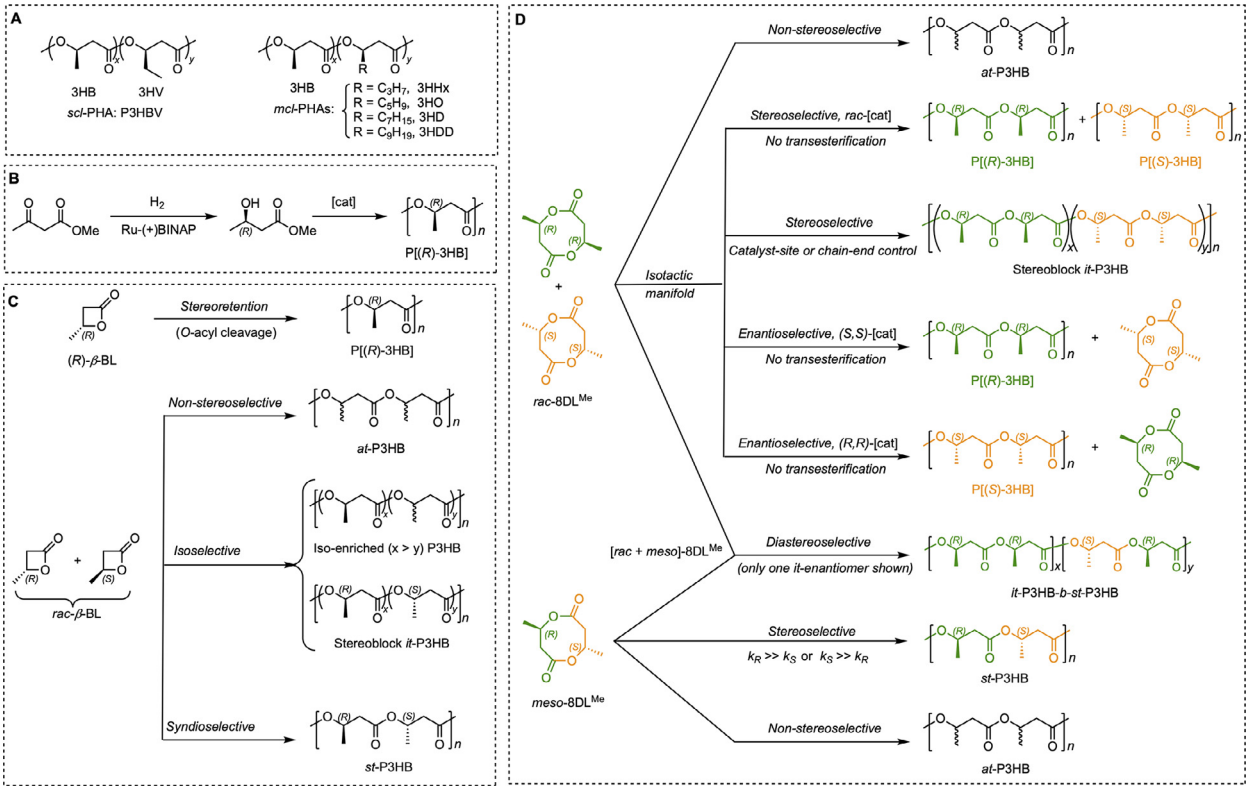

Fig. 1. Representative common biological PHAs as copolymers: 3HB = 3-hydroxybutyrate, 3HV = 3-hydroxyvalerate, 3HHx = 3-hydroxyhexanoate, 3HO = 3-hydroxyoctanoate, 3HD = 3-hydroxydecanoate, 3HDD = 3-hydroxydodecanoate (A) and three major chemocatalytic routes towards PHAs, represented by P3HB materials with various tacticities: (B) step-growth polymerization, (C) chain-growth polymerization by ROP of four-membered β-BL, (D) carbonylative polymerization, and (E) chain-growth polymerization by ROP of eight-membered dimethyl diolide (*rac*-8DL^{Me} and *meso*-8DL^{Me}).

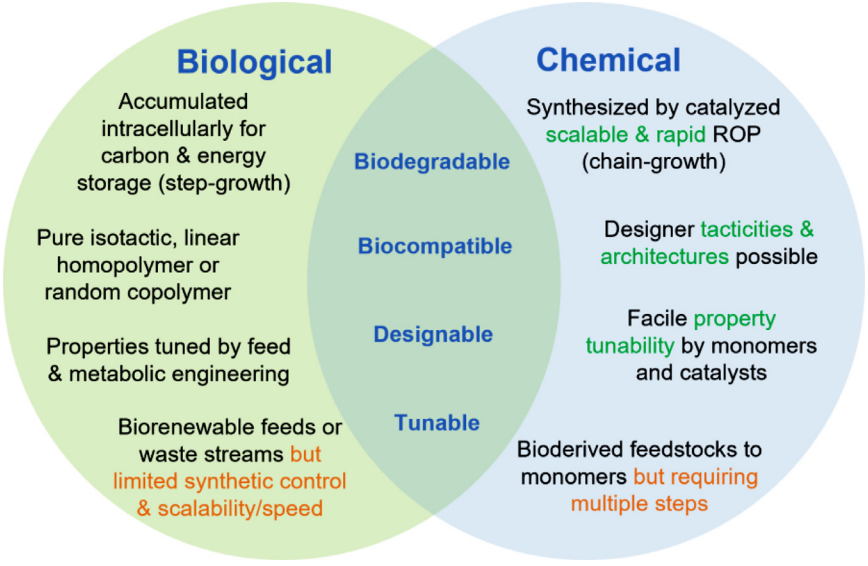

Fig. 2. Differentiating and overlapping features of biological and chemical routes to PHAs.

(rac) and *R,S meso*), allowing access to a more diverse set of possible stereomicrostructures (E, Fig. 1).

This review intends to focus on the chemocatalytic routes towards PHAs, including investigations of the various stereomicrostructures that can be accessed through different catalytic ROP strategies, the design of different organometallic and organic catalysts to synthesize P3HB, as well as the controlled synthesis of various homo- and copolymer PHAs that are either challenging to produce or inaccessible through biological pathways. Several recent reviews offer complementary perspectives that explore discrete metal catalysts for the ROP of cyclic esters in general to various stereomicrostructures [40–46], but this review focuses on PHAs, poly(3-hydroxyacid)s, specifically, encompassing and analyzing all of the three chemocatalytic routes towards various types of PHA materials.

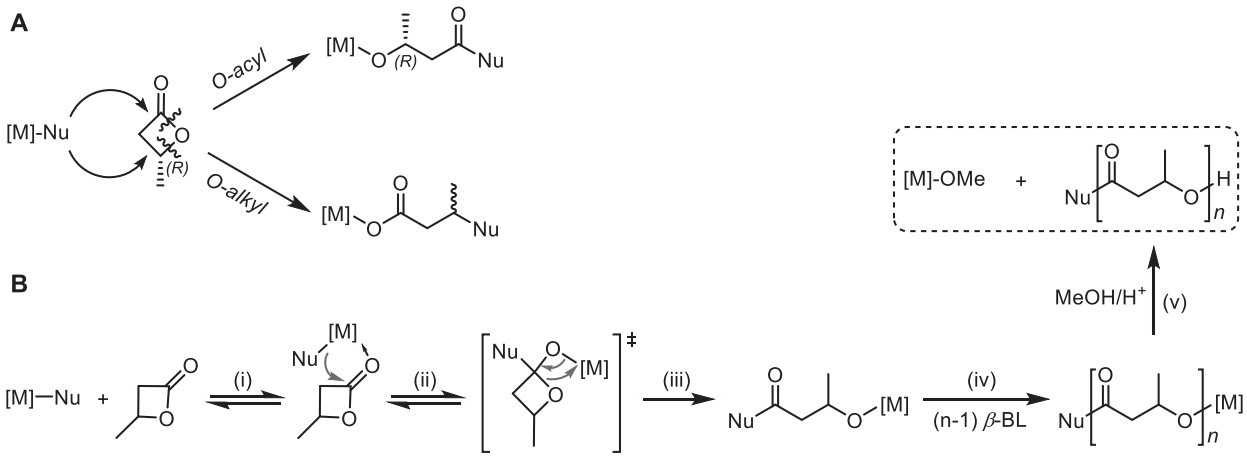

Scheme 1. (A) General mechanism of ring-opening of β-BL resulting in stereo-retention via *O*-acyl bond cleavage and chiral inversion or racemization via *O*-alkyl bond cleavage. [M] denotes a metal-based catalyst center and Nu a nucleophile, typically an alkoxy or amide ligand. (B) Generally accepted coordination-insertion mechanism for the ROP of β-BL using metal-based catalysts. [M] denotes a metal-based catalyst center and Nu a nucleophile, typically an alkoxy or amide ligand.

2. Isotactic P3HB

2.1. Mechanistic considerations

The desire to make a synthetic analog to bacterial derived, perfectly *it*-P3HB has inspired research efforts spanning 60+ years since the initial report on the ROP of β-BL in 1961 [47]. It has been well-established by now that the most facile synthetic approach towards high-molecular-weight polyesters is the ROP of cyclic esters (or lactones). For the synthesis of P3HB, the simplest lactone monomer is the highly strained, four-membered β-BL. There are two general mechanistic pathways for ring-opening of β-lactones: *O*-acyl bond cleavage or *O*-alkyl bond cleavage (Scheme 1, A). The former allows the stereo-retention of the chirality at the β-carbon, while the latter leads to either chiral inversion or racemization at the chiral center. It is generally accepted that the metal-mediated ROP of β-BL (or other cyclic esters) proceeds through the classic coordination-insertion mechanism, involving the following key fundamental steps: (i) monomer coordination to the metal catalyst center; (ii) nucleophilic attack of the coordinated monomer by the nucleophilic ligand (Nu) on the metal to form the tetrahedral intermediate; (iii) ring-opening of the intermediate via concerted C–O and [M]–O bond breaking/forming events to generate the Nu–[3HB]-O–[M] propagation species; (iv) repeated monomer additions through the same coordination-insertion cycle to the propagating species, producing the P3HB chains; and (v) quenching of the propagating chain to the P3HB with Nu/H chain ends (Scheme 1, B).

As β-BL has one stereogenic center, it is available in either an enantiopure or *rac* form. A convenient, albeit expensive, strategy to produce purely isotactic, optically active *it*-P3HB is to use the enantiopure form of β-BL, thereby avoiding the need to control the stereoselectivity of the polymerization, provided that the ROP proceeds via *O*-acyl bond cleavage (C, Fig. 1) [48–51]. The most common termination pathway is through formation of crotonate end groups, resulting in generation of low-molecular-weight polymers and undesirable, non-biomimetic end groups (Scheme 2) [2].

2.2. ROP of β-BL

Agostini *et al.* first reported the polymerization of (*R*)-β-BL with the $AlEt_3/H_2O$ mixture [52]. The polymerization was presumed to proceed via the *O*-acyl bond scission because the stereochemistry was retained resulting in optically active P[(*R*)-3HB]; however, due to the poorly resolved monomer (~73% optical clarity) the resulting polymer had lower optical activity compared to biologically derived P3HB [50]. Lenz hypothesized a route towards P[(*R*)-3HB] by inversion of stereochemistry via ROP of (*S*)-β-BL;[48] with the $AlEt_3/H_2O$ initiator, the inversion of stereochemistry was observed, which is opposite to what Shelton *et al.* observed [50]. These conflicting results highlight the lack of control over this catalyst structure and thus the polymer stereochemistry by the non-discrete AlR_3/H_2O system. Lenz also used $ZnEt_2/H_2O$ as the initiator for ROP of (*S*)-β-BL but observed retention of stereochemistry to give P[(*S*)-3HB] [48]. Tanahashi and Doi polymerized chiral β-BL of different enantiomeric excess using $ZnEt_2/H_2O$ and obtained *it*-diad fractions, with P_m (defined as the probability of *meso* linkages between two consecutive monomer units) up to 0.85, thanks to retention of the original *S* and *R* configurations of the β-BL monomer. This *it*-polymer showed a T_m of 135 °C and an enthalpy of fusion (ΔH) = 64.3 J/g [53]. By comparison, the biologically produced P3HB has T_m ~ 170 °C and ΔH ~ 80 J/g. Kemnitzer *et al.* employed the similar strategy using $ZnEt_2/H_2O$ and produced various stereo-copolymers by adjusting the enantiopurity of the β-BL monomer [54].

Even with the chiral β-BL monomer, achieving synthetic analogs of the biologically derived P3HB via the ROP is not straightforward due to competing *O*-acyl and *O*-alkyl bond cleavage pathways (*vide supra*). In one example, a distannoxane complex initiated the ROP of (*R*)-β-BL, proceeding via the *O*-acyl bond cleavage with retention of configuration and thus producing P[(*R*)-3HB] (**1**, Fig. 3) [55]. Ring-opening copolymerization of (*R*)-β-BL with ε-caprolactone, γ-valerolactone, β-methyl-γ-valerolactone, and L-lactide by such a distannoxane complex yielded copolyesters of high M_n (> 100 kg/mol comprising mostly (*R*)-3-hydroxybutyrate units) [56]. ROP of (*R*)-β-BL mediated by potassium alkoxide crown ether complexes proceed via stereoinversion (i.e. *O*-alkyl bond cleavage) to afford *it*-poly[(*S*)-3HB] [49]. This finding led to the synthesis of P[(*R*)-3HB] with a high P_m up to 0.95 through regioselective anionic polymerization of (*S*)-β-BL using (*R*)-3-hydroxybutyric acid sodium salt and 18-crown-6 ether initiator (**2**, Fig. 3) via *O*-alkyl-bond scission with an inversion of stereochemistry [51]. Overall, the methods of polymerizing chiral β-BL to biomimetic *it*-P3HB by the anionic ROP remained largely ineffective, due to often competing stereo-retention vs inversion pathways, and also produced *it*-P3HB with relatively low molecular weights (typically M_n ~ 10 kg/mol).

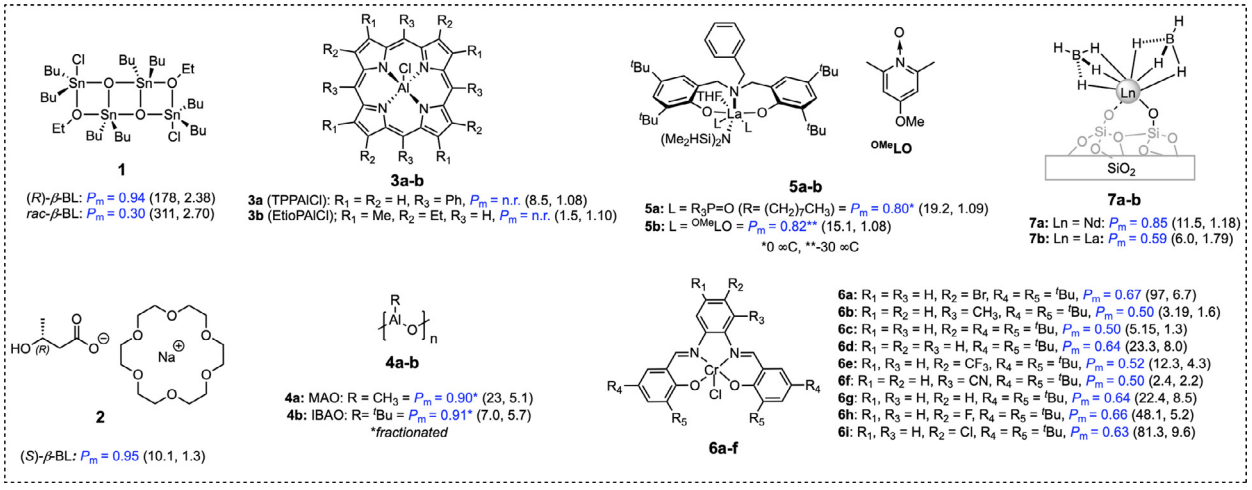

Fig. 3. Catalyst or initiator systems that produced isotactic or iso-rich P3HB (P_m <0.85, except for ROP of enantiopure (*R*)-β-BL) from the ROP of *rac*-β-BL. (n.r. = not reported in the original literature). M_n in kg/mol and $Đ$ values are placed in parentheses for each system.

A more economical but challenging route to produce *it*-P3HB is the stereoselective polymerization of *rac*-β-BL. A number of organometallic compounds have been employed in this endeavor since the first example of the ROP of *rac*-β-BL to a "powdered polymer" by $ZnEt_2/O_2$ was reported by Inoue in 1961 [47]. One of the first examples of stereoselective polymerization of *rac*-β-BL was enabled by the use of a coordinative alkyl aluminum complex (formulated as Et_2Al•O•CPh:NPh) which yielded a mixture of iso-enriched and *at*-polymer materials [57]. This mixture was then fractionated with acetone to give the insoluble, crystalline *it*-fraction that had high T_m values of 167–169 °C. Although this method produced the crystalline *it*-P3HB, it also afforded large fractions of soluble, *at*-polymer and took up to 7 days at 60 °C to achieve appreciable polymer yields. There are several examples of using mixtures of trialkylaluminum complexes, especially triethylaluminum, with water to polymerize *rac*-β-BL over several days to fractions of the crystalline, relatively high molecular weight polymer that was thermally similar to that of biologically produced P3HB, plus large fractions of soluble, low molecular weight polymer products [52,58,59]. The isotacticity of the P3HB produced by trialkylaluminum complexes was quantitatively characterized by ^{13}C NMR [60]. The acetone insoluble crystalline fraction had a P_m up to 85%, T_m values of 165–170 °C, and a high ΔH up to 95 J/g.

Subsequent efforts seeking to achieve *it*-P3HB from the ROP of *rac*-β-BL focused on the development and utilization of well-defined, discrete catalyst or initiator systems. In this context, aluminum porphyrins, such as (tetraphenylporphinato)(TPP)aluminum chloride (TPPAlCl) (**3a**, Fig. 3), were found to mediate living ROP of β-BL, but these catalysts suffered from very low activity, requiring 6 days to reach quantitative monomer conversion at room temperature to yield only low-molecular-weight polymer (M_n = 8.5 kg/mol) [61]. Changing the porphyrin from TPP to etioporphyrin (EtioP) (**3b**, Fig. 3) further reduced the activity and the polymer molecular weight [62]. Although the tacticity of the resulting polymer was not described, it was hypothesized the mechanism of initiation resulted in loss of control of the stereogenic center: the chloride of TPPAlCl was proposed to attack the β-carbon of the monomer which leads to lactone insertion through *O*-alkyl bond scission [62], and this resulting carboxylate anion propagates via the *O*-alkyl bond scission to regenerate the porphinatoaluminum carboxylate [61]. Despite the ability to mediate the living ROP of β-BL, aluminum porphyrin complexes are poor catalysts in terms of activity and stereoselectivity.

Methylaluminoxane (MAO) (**4a**, Fig 3) and isobutylaluminoxane (IBAO) (**4b**, Fig. 3), commonly employed as co-catalysts in the metal-catalyzed olefin polymerization [63], were also utilized to initiate the ROP of *rac*-β-BL [64]. Despite the need for high catalyst loadings (10 mol%), the ROP led to 60% of the crude polymer product being the insoluble, crystalline (T_m = 163 °C and ΔH = 21 J/g) polymer fraction with P_m ranging between 0.78–0.91 [64].

Polymerization of *rac*-β-BL with chiral initiators, such as a complex of *R*(-)-3,3-dimethyl-1,2-butanediol and $ZnEt_2$, resulted in the partial kinetic resolution of the racemic monomer because the catalyst preferentially polymerizes (*R*)-β-BL to P[(*R*)-3HB] and leaves (*S*)-β-BL partially resolved (Scheme 3) [65]. Initiation and propagation proceed via *O*-acyl bond cleavage thus retaining stereoconfiguration of the enchained monomer. The insoluble fraction of the resulting polymer showed two endotherms with T_m = 122 °C and 166 °C by differential scanning calorimetry (DSC), and the latter predominant crystalline fraction indicates the presence of an extended distribution of *it*-sequences ($P_m \sim 0.75$). Noteworthy also is that this catalyst system was much more active than the previous Al or Zn systems (often mixed with water or common alcohol) – achieving up to 84% conversion at room temperature in 5.5 h. Different metal alkyls including $AlEt_3$ and $CdMe_2$ were also studied; $AlEt_3$ had drastic reduction in activity (13% polymer yield after 18 days of reaction) but maintained the stereoselectivity, while $CdMe_2$ was much more reactive but preferentially produced the opposite enantiomeric poly[(*S*)-3HB] [65].

Mixing alkyl aluminum and zinc complexes with water or alcohol often resulted in formation of oligomeric species or non-discrete complexes. To address this issue, Zintl *et al.* employed discrete chromium salophen complexes (**6**, Fig. 3) for the ROP of *rac*-β-BL and achieved appreciable isoselectivities (P_m up to 0.66) [66]. These complexes produced moderately isotactic polymers due to the binuclear mechanism involved that preferentially allows entry of an incoming β-BL enantiomer based on the stereoconfiguration of the previous enchained enantiomer (i.e., chain-end control). Adding a halogen to the bridging phenyl ring improved activity and selectivity of the polymerization as well as molecular weight of P3HB substantially. For example, fluorination at the 4-position (**6b**, Fig. 3) yielded a catalyst that is not only twice as active as the non-halogenated derivative, but also produced P3HB with M_n (48.1 kg/mol) which is twice the weight of the P3HB produced by the parent catalyst. Chlorination (**6c**, Fig. 3) showed the similarly enhanced activity and further increased M_n to 81.3 kg/mol, but the dispersity of the resulting P3HB is very high ($Đ$ = 9.6) [66].

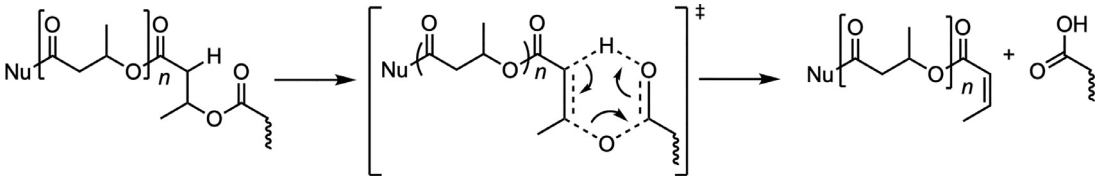

Scheme 2. A common termination pathway in chemocatalytic synthesis of P3HB from β-BL, which leads to crotonate end group formation.

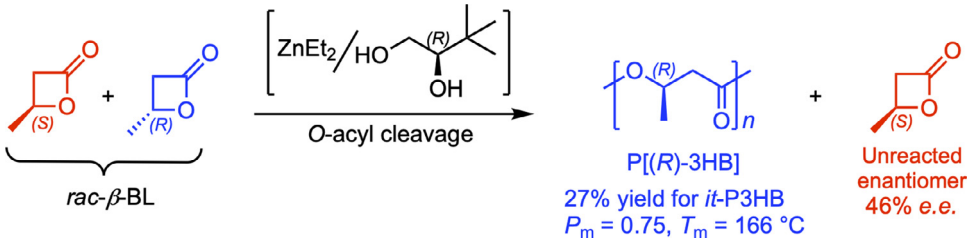

Scheme 3. Partial kinetic resolution polymerization of *rac*-β-BL with a chiral Zn-based initiator system comprising *R*(-)-3,3-dimethyl-1,2-butanediol and $ZnEt_2$.

Reichardt *et al.* further explored these profound electronic effects and found that, while electron withdrawing halogens, such as Br (**6a**, Fig. 3), increased reactivity, electron donating groups such as methyl (**6b**, Fig. 3) and *tert*-butyl (**6c**, Fig. 3) completely inhibited polymerization, relative to the parent model catalyst (**6d**, Fig. 3) [67]. This activity inhibition was attributed to increasing the electron density on the Lewis acidic metal center which weakens the Lewis acid bonding to monomer and the growing polymer chain [67]. The use of strongly electron withdrawing groups such as CF_3 (**6e**, Fig. 3) and CN (**6f**, Fig. 3) also decreased activity because of enhancing chain affinity towards one catalyst center thus hindering transfer of the activated monomers to the second complex [67]. Further study revealed these chromium complexes even transformed *in situ* into a heterogeneous catalytic process [68], which can also explain the formation of the polymer with high dispersity values. More specifically, the Cr complex crystalizes into a polymeric form during polymerization, which allows for fast, enantiomorphic, bimetallic or multinuclear stereoinduction of *rac*-β-BL by specially arranged chromium centers. It was also suggested that water is important, not as a chain transfer agent but in the formation of the active polymeric chromium species. Changing the ligand substituents alters the complex's ability to transform into the polymeric form and thus reduces activity. Although the polymers with relatively high molecular weights could be achieved, they were accompanied by high dispersities, because of the continual initiation of new polymer chains by newly generated catalyst centers during propagation [68].

Recently, a benzyl-substituted amino-bisphenolate lanthanum complex (**5**, Fig. 3) was found to increase the reactivity and isoselectivity of the ROP of *rac*-β-BL, upon addition of a neutral achiral donor ligand [69]. Use of an electron-rich phosphine oxide donor ligand, in particular trioctylphospine oxide ($R_3P{=}O$), resulted in the formation of iso-rich P3HB (P_m = 0.80) when the reaction temperature was reduced to 0 °C (**5a**, Fig. 3) [69]. Switching the neutral donor ligand to *N*-oxides, specifically ^{OMe}LO, promoted enhancements in both activity and isoselectivity in the ROP of *rac*-β-BL to P3HB, achieving P_m = 0.82 when reaction temperature was -30 °C (**5b**, Fig. 3) [70].

A more common way of generating a heterogenous catalyst system is through anchoring of a molecular catalyst onto an inorganic support. In this context, lanthanide borohydrides were supported on silica, and the resulting heterogenous catalyst was examined for the ROP of *rac*-β-BL [71]. Specifically, a grafted neodymium borohydride complex, $Nd(BH_4)_3(THF)/SiO_2$ (**7a**, Fig. 3), exhibited good activity (82% monomer conversion in 24 h) and stereoselectivity (P_m = 0.85). The corresponding lanthanum complex with a large ionic radius, $La(BH_4)_3(THF)/SiO_2$ (**7b**, Fig. 3), showed poor activity and also lower stereoselectivity (P_m = 0.59). Worth noting here is that the trend for the molecular catalysts performed in solution is often the opposite. In comparison, the (unsupported) molecular version of these complexes led to totally *at*-polymer.

2.3. ROP of rac-8DL^{Me}

Achieving P3HB with high isotacticity (P_m > 0.90 for the bulk polymer without fractionation) remained elusive until 2018 when Tang and Chen developed a new chemocatalytic route to P3HB via the ROP of a *rac*-diolide, the 8-membered cyclic dimer of 3-hydroxybutyrate (*rac*-8DL^{Me}), to perfectly *it*-P3HB (P_m > 0.99) (Fig. 4) [72]. The increased sterics present in *rac*-8DL^{Me} relative to *rac*-β-BL and the realized right substrate/catalyst matching are hypothesized to be the causes for the higher degree of stereochemical control (thus production of highly isotactic P3HB) in the catalyzed ROP of *rac*-8DL^{Me}. The ROP of *rac*-8DL^{Me} was evaluated using a series of discrete, molecular catalysts including $La[N(SiMe_3)_2]_3$ (**8**, Fig. 4) and yttrium amido complexes supported by tetradentate [O^-,*N*,*O*,O^-] ligands (**9-10**, Fig. 4). These complexes had been utilized for other ROP reactions [12,73,74] and their use to polymerize *rac*-β-BL to *st*-P3HB [75–77] will be discussed in Sections 3.1.2 and 5.2. The investigation of the steric, electronic, and symmetry effects of the salen-ligand framework (*rac*-**11a-b**, **11e**, Fig. 4) highlighted the ideal match between the C_2-symmetric, trityl-*ortho*-substituted salen ligated yttrium complex and *rac*-8DL^{Me} resulting in the formation of essentially stereo-perfect *it*-P3HB (*rac*-**11d**, Fig. 4). This *it*-P3HB had a high T_m of 171°C and ΔH ~80 J/g, thus exhibiting the high crystallinity and thermal properties similar to those of the microbial P3HB [72].

Further investigation into the stereocontrol of the ROP revealed an enantiomorphic-site control mechanism, pointing to the possibility of kinetic resolution of *rac*-8DL^{Me} if an enantiomerically pure catalyst is used. Indeed, the polymerization of *rac*-8DL^{Me} with enantiopure (*R*,*R*)-**11d** resulted in 50% conversion of the monomer where all of the (*S*,*S*)-8DL^{Me} was polymerized to P[(*S*,*S*)-3HB], leaving (*R*,*R*)-8DL^{Me} unreacted. For typical kinetic resolution polymerization, the reaction needs to be monitored and stopped manually when the monomer conversion approaches ~50%, thereby avoiding

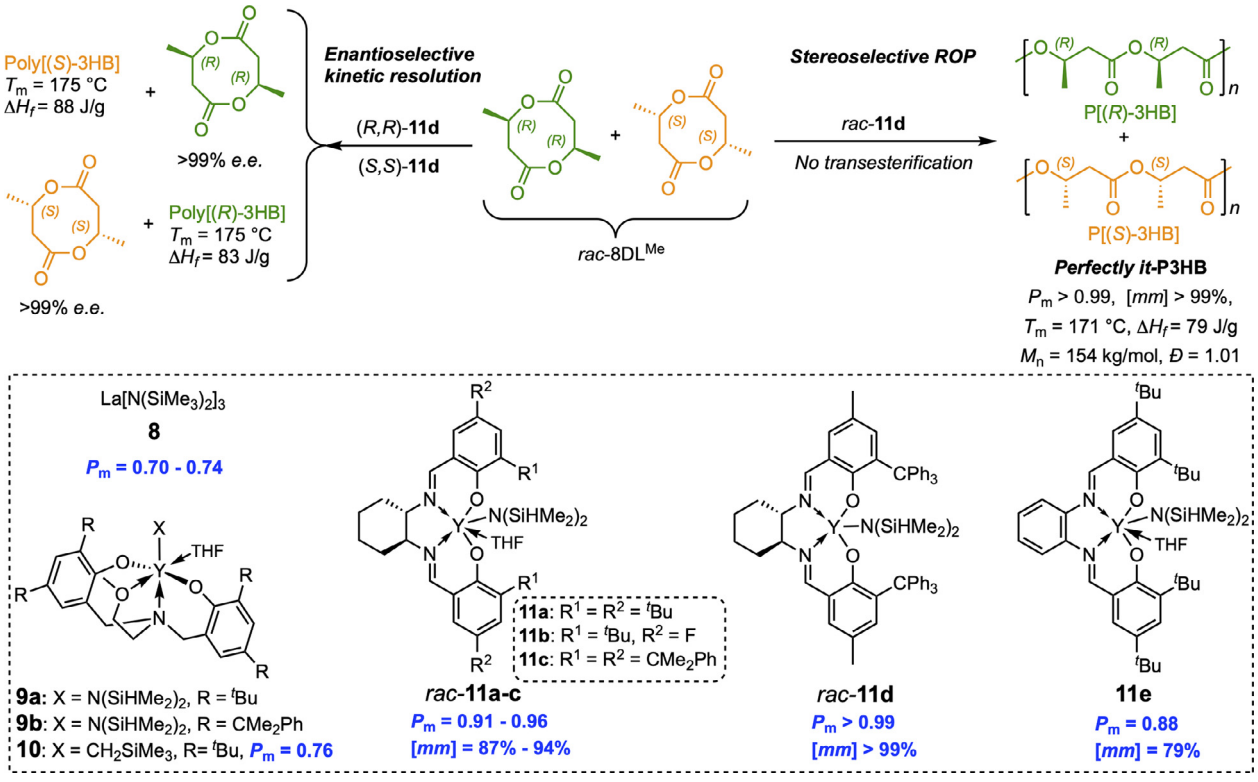

Fig. 4. Stereoselective ROP and enantioselective kinetic resolution polymerization of *rac*-8DL^{Me} by discrete chiral and non-chiral lanthanum and yttrium complexes.

stereo-tapering when the concentration factor of the slow-reacting enantiomer overrides the kinetic preference of the fast-reacting enantiomer with its concentration diminishes as the reaction progresses. If the reaction is allowed to continue to completion, then a stereo-tapered diblock copolymer is typically produced. Fascinatingly, the polymerization of *rac*-8DL^{Me} by (*R,R*)-**11d** automatically stopped at 50% monomer conversion, without further incorporating the other enantiomeric monomer that would lead to a stereodiblock or stereo-tapered BCPs, thus achieving essentially perfect enantioselectivity in the kinetic resolution polymerization (Fig. 4) [72]. When enantiopure (*S,S*)-**11d** was employed, the ROP of *rac*-8DL^{Me} gave the results of mirror-image products: P[(*R,R*)-3HB] and (*R,R*)-DL^{Me} (Fig. 4). The resulting pure *it*-P3HB exhibited a high T_m up to 175 °C, essentially identical to that the microbial P3HB, but the synthetic P3HB by the ROP exhibits extremely narrow *Đ* values (<1.03), relative to typically high *Đ* values (> 2.0) of the biological P3HB [72]. The synthetic P3HB with a narrow *Đ* value showed a much narrower crystallization peak and also a smaller [T_m - T_c] window than that of bacterial P3HB, implying faster crystallization; however, the overall crystallinity is essentially the same [72]. A recent study that compared crystallization behaviors of the synthetic racemic P3HB of varying molecular weights and biologically-derived P[(*R*)-3HB] observed that the enantiomeric purity is the dominating factor in crystallization kinetics [78].

When *rac*-8DL^{Me} is polymerized by a racemic catalyst such as *rac*-**11d**, the resulting *it*-P3HB was shown to be a mixture of enantiomeric polymers P[(*R*)-3HB] and P[(*S*)-3HB] (Scheme 4), thanks to the complete enantioselectivity of (*R,R*)-catalyst for addition of (*S,S*)-8DL^{Me} and (*S,S*)-catalyst for addition of (*R,R*)-8DL^{Me} and no transesterification upon full monomer conversion. Note that transesterification would lead to stereo(multi)block copolymer. This methodology is an important leap forward in discovering a scalable chemocatalytic route towards biomimetic P3HB.

3. Syndiotactic P3HB

3.1. ROP of rac-β-BL

3.1.1. Sn-based initiators

Although microorganisms produce exclusively *it*-P3HB, chemocatalytic ROP of *rac*-β-BL can produce unnatural *st*-P3HB. Throughout the 1990s, Sn complexes were examined for the ROP of *rac*-β-BL because they had been shown to be active in the polymerization of various lactones [79,80]. The use of $^{n}Bu_3Sn$-OCH_3 (**12a**, Fig. 5) led to a notable preference for *st*-placement, P_r (defined as the probability of *rac* linkages between monomer units) up to 0.70, but the activity was extremely low [81]. Room temperature polymerization required 55 days to achieve only 37% yield; while increasing the temperature to 90°C reduced the reaction time to 13 days, this condition consequently decreased the stereoselectivity (P_r = 0.61), yielding the syndio-enriched P3HB with a low T_m of only ~50 °C.

Different Sn(IV) complexes were employed for tuning the syndioselectivity of the ROP of *rac*-β-BL. Using $^{n}Bu_2Sn(OMe)_2$ (**12b**, Fig. 5), $(^{n}Bu_3Sn)_2O$, and $(Ph_3Sn)_2O$ (**13a** and **13b**, Fig. 5) under various conditions reached a maximum P_r value of 0.83 when the polymerization temperature was lowered to -17°C [81–83]. The activity of these complexes was extremely low, however, taking 13 to 75 days of reaction time when the reaction was carried out at this temperature for the highest P_r value [82]. The observed syndioselectivity was attributed to be resulted from the asymmetry of the chain end coordinated to the respective Sn catalysts, thus a chain-end control mechanism [83].

Use of cyclic dibutyltin resulted in noticeably higher molecular weights but the syndiotacticity remained only modest (P_r = 0.62) [84]. Polymers with higher molecular weights (M_n up to 80 kg/mol) and syndiotacities (P_r up to 0.72) were obtained with dialkyltin(IV) oxides, $R_2Sn{=}O$, in particular when R = ^{n}Bu (50 °C)

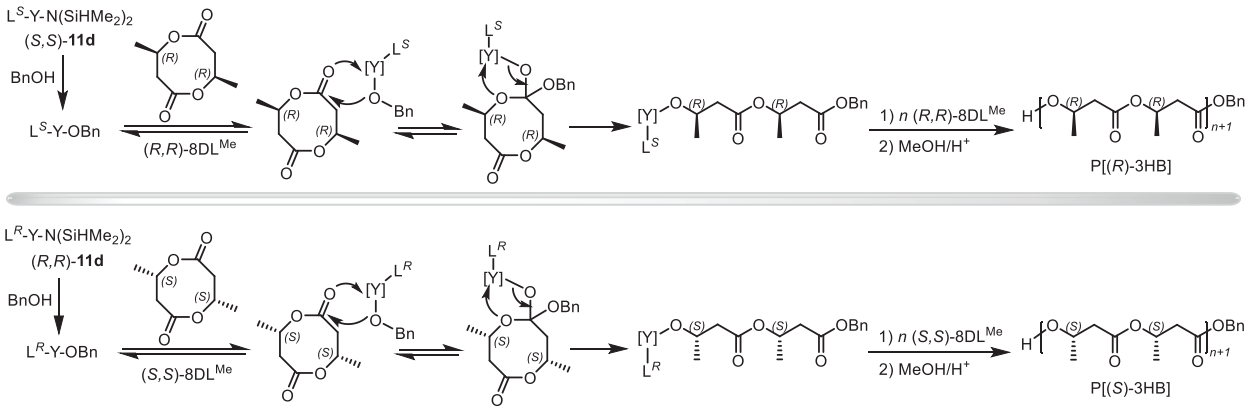

Scheme 4. Outlined fundamental steps proposed for the stereoselective ROP of *rac*-8DL^{Me} by the racemic catalyst, ***rac*-11d**, to produce a mixture of enantiomeric P[(*R*)-3HB] and P[(*S*)-3HB].

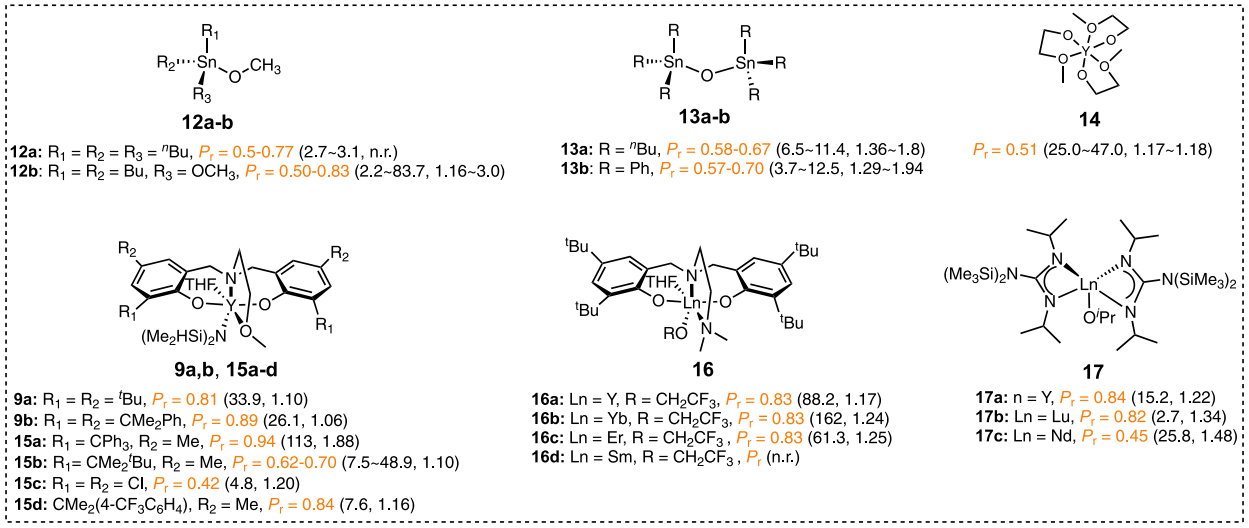

Fig. 5. Catalyst or initiator systems that produced syndiotactic or syndio-rich P3HB from the ROP of *rac*-β-BL (n.r. = not reported). M_n in kg/mol and $Đ$ values are placed in parenthesis for each initiator.

and Et (100 °C) [85]. As distannoxane complexes (**1**, Fig. 3) were found to polymerize (*R*)-β-BL with retention of stereochemistry to form *it*-P3HB [56], they were also utilized for the ROP of *rac*-β-BL to give syndio-enriched P3HB (P_r = 0.67), attributed to the steric control resulted from diastereomeric interactions between the Sn-coordinated P3HB chain ends and the incoming enantiomeric β-BL monomers [86].

3.1.2. Rare-earth metal catalysts

As can be seen from the above selected examples of the initiator systems, classical organometallic complexes of Zn, Al, and Sn are sluggish and often require high temperatures to bring about useful activities for either isoselective or syndioselective ROP of β-BL. Discrete, rare-earth metal-based molecular catalysts have been shown to exhibit exceptional efficiency and activity in the ROP of ε-caprolactone and lactide under mild conditions and, naturally, such catalysts were employed to polymerize β-BL [40,42]. Le Borgne *et al.* in 1994 polymerized *rac*-β-BL with yttrium 2-methoxyethoxide (**14**, Fig. 5) and achieved high activity (100% conversion in 20 min at room temperature) and living polymerization characteristics, including the preparation of homopolymers and well-defined BCPs with lactide [87]. The resulting P3HB was shown to be atactic, however, based on NMR analysis.

Carpentier and co-workers subsequently explored multi-dentate ancillary ligands to tune the catalytic properties of the rare-earth metal complexes, minimize catalyst aggregation, and limit transesterification reactions, thereby enhancing activity and stereochemical control [40,42]. In particular, yttrium bis(dimethylsilyl)amido and bis(trimethylsilyl)methyl complexes supported by a tetradentate bis(phenoxy) ligand (**9a** and **9b**, Fig. 4 and **15a–d**, Fig 5.) [88] have been shown to be highly active and efficient catalysts for syndioselective polymerization of *rac*-β-BL. With a bulky cumyl group placed at the position ortho to the phenoxy oxygen (**9b**, Fig. 5), this well-defined, C_s-symmetric single-site bis(phenolate) yttrium complex converted *rac*-β-BL in toluene at -20°C to highly *st*-P3HB (P_r = 0.94, M_n = 113 kg/mol, $Đ$ = 1.88) [76]. The less sterically encumbered yttrium complex with *tert*-butyl group at the ortho position (**9a**, Fig. 5) displayed an appreciable loss in stereoselectivity (P_r = 0.81). Changing the temperature and/or concentration of the polymerization reaction notably affected the activity and selectivity of the ROP. The highly *st*-P3HB (P_r= 0.94) exhibited a high T_m of 178 °C [76].

The impressively high syndioselectivity was further investigated by close analysis of the steric and electronic effects of this class of methoxy-amino bis(phenolate)-yttrium complexes (with the appendant *ether* side arm) on their activity, syndioselectivity, and living behavior (Fig. 6) [75]. It was discovered that, when bulky,

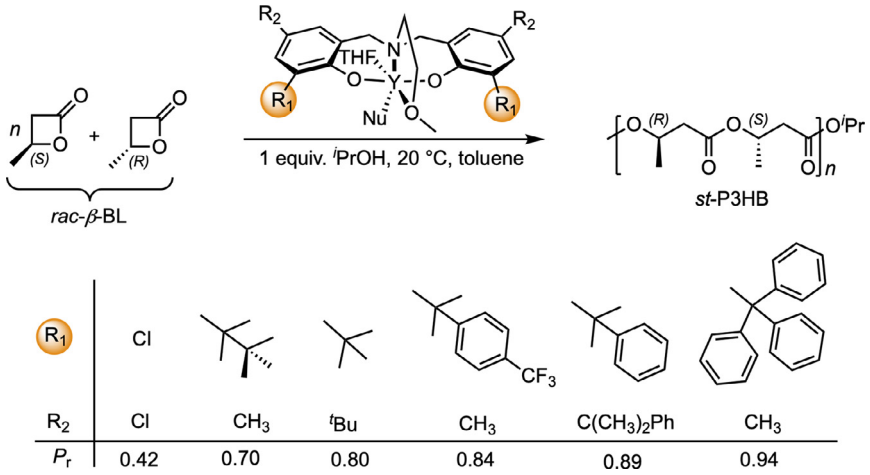

Fig. 6. Syndioselective polymerization of *rac*-β-BL in toluene by C_s-symmetric catalysts 15 to *st*-P3HB with various degrees of syndiotacticity as a function of ortho-substituents on the bis(phenolate) rings.

aryl-containing substituents are placed at the *ortho* positions, steric interactions are involved, and the P_r value was increased compared to sterically smaller substituents. For example, when running the polymerization at 20°C in toluene, switching from the cumyl substituted complex (**9b**, Fig. 5) to trityl substituted analog (**15a**, Fig. 5) enhanced the syndiotacticity considerably from P_r = 0.89 to P_r = 0.94. Alkyl *ortho* substituents, including those that are rather bulky, gave lower P_r values (**9a** and **15b**, Fig. 5). Electron withdrawing Cl substituents resulted in loss of stereoselectivity (**15c**, P_r = 0.42, Fig. 5). Introducing a para-trifluoromethyl group on the phenyl ring of the cumyl substituent (**15d**, Fig. 5) achieved higher stereoselectivity than the *tert*-butyl substituent (**9a**, Fig. 5), most likely due to increasing sterics, but placing this electron-withdrawing group on the cumyl phenyl ring lowered stereoselectivity compared to the parent cumyl complex (P_r = 0.84 vs. P_r = 0.89, Fig. 6) [75]. The beneficial effect of the phenyl group in *ortho* substituents prompted further investigation by DFT calculations, indicating C-H–π interactions between one methylene hydrogen of the 3-hydroxybutyrate moiety and the *ortho* and *meta* carbon atoms of a phenyl ring of the cumyl (-Me_2Ph) substituent which appeared as the most stable structure [75].

The previously described studies [75,76] showed that ligand substituents are essential for stereochemical control through a chain-end control mechanism and that the ROP of *rac*-β-BL by metal alkoxides can proceed via a coordination-insertion mechanism or an anionic mechanism. However, the ROP by these bis(phenolate) yttrium complexes proceeds via a coordination-insertion mechanism; as a result, there was no clear crotonate formation (*c.f.*, Scheme 2) which would indicate an anionic mechanism [76]. Further mechanistic investigation elucidated a chain-end-control mechanism responsible for the resulting stereochemistry [77].

Cai *et al.* also synthesized a series of neutral amine-bridged bis(phenolate)-lanthanide alkoxide complexes (**16**, Fig. 5) for the ROP of *rac*-β-BL. These complexes with the appendant *amine* side arm effected a controlled polymerization to produce *st*-P3HB with narrow $Đ$ values (<1.25) and P_r = 0.83. The ROP carried out in toluene showed higher activity and syndioselectivity, as compared to the ROP in coordinating solvent THF. The size of ionic metal radii had no notable effects on stereoselectivity, but it did affect the catalytic activity, with Yb > Er > Y >> Sm (**16a-d**, Fig. 5) [89]. The influence of bimetallic complexes on stereoselectivity was also investigated and similar activity and selectivity were observed [90]. Furthermore, bis(guanidinate) alkoxide complexes of lanthanides (**17**, Fig. 5) were employed for the ROP of *rac*-β-BL. Complexes of group 3 metals with smaller atomic radii (Y and Lu) were active and produced *st*-P3HB with P_r up to 0.84 (**17a** and **17b**, Fig. 5) [91]. The neodymium complex (**17c**, Fig. 5) was also active, but it lacked stereoselectivity and produced *at*-P3HB. Combining both the guanidinato and bis(phenolate) ligands for the metal center did not enhance polymerization activity [92].

3.2. *ROP of* meso-*8DL^{Me}*

Another route to *st*-P3HB is via the stereoselective ROP of *meso*-8DL^{Me}, which is the diastereomeric co-product in the synthesis of *rac*-8DL^{Me} and generally discarded in favor of *rac*-8DL^{Me} that is utilized to produce *it*-P3HB. As described above, the ROP of *rac*-8DL^{Me} results in perfectly *it*-P3HB, thanks to the enantiomorphic site control by the C_2-symmetric, chiral salen-ligated yttrium complexes. These results suggested that such racemic catalysts should also be stereoselective toward *meso*-8DL^{Me}, as the (*R,R*)-catalyst should selectively ring-open *meso*-8DL^{Me} at the (*S*)-site of the ester (*O*-acyl) bond while the (*S,S*)-catalyst should selectively cleave the ester bond of *meso*-8DL^{Me} at the (*R*)-site, thus affording *st*-P3HB (Scheme 5). Indeed, the catalyst with the bulky, trityl-substituted ligand complexed to the larger lanthanum ion (**11f**, Scheme 5) showed good activity and high syndioselectivity, affording *st*-P3HB with a high T_m of 170°C and P_r up to 0.92 [93].

4. Atactic P3HB

4.1. *Organocatalytic ROP of* rac-β-*BL*

Metal-free approaches to polyesters via the ROP of cyclic esters are important for accessing metal-free polyesters specifically for microelectronics and biomedical applications, which can also take advantage of mechanistic pathways unique to organocatalysts [94,95]. In 2002, Hedrick and co-workers first reported the organic ROP of cyclic esters using *N*-heterocyclic carbenes (NHCs) as catalysts [96]. In that communication, the authors included one example that 1,3-bis(2,4,6-trimethylphenyl)imidazole-2-ylidene (IMes, **19**, Fig. 7) effectively polymerizes *rac*-β-BL to *at*-P3HB with a narrow $Đ$ (1.15).

Another NHC, TPT (1,3,4-triphenyl-4,5-dihydro-*1H*-1,2,4-triazol-5-ylidene) (**20**, Fig. 7), together with methanol, was employed for the ROP of *rac*-β-BL at 80°C, yielding an uncontrolled polymerization due to both postulated alkoxide and carboxylate initiation pathways (Scheme 6) [97,98]. The basicity of the NHC was also attributed to some undesired elimination reactions with unreacted

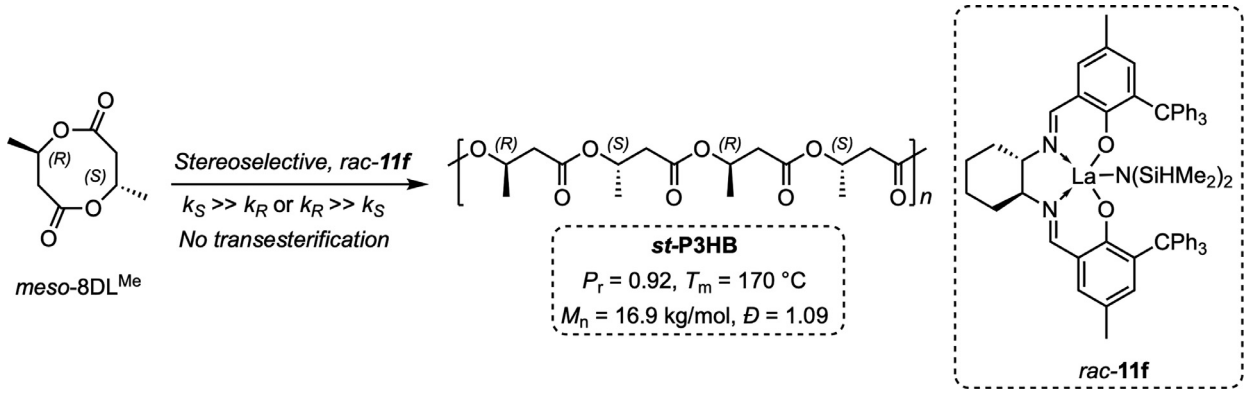

Scheme 5. Stereoselective ROP of *meso*-8DL^{Me} to *st*-P3HB by racemic catalyst *rac*-**11f** rendered by the catalyst-controlled enantiomeric-site selectivity.

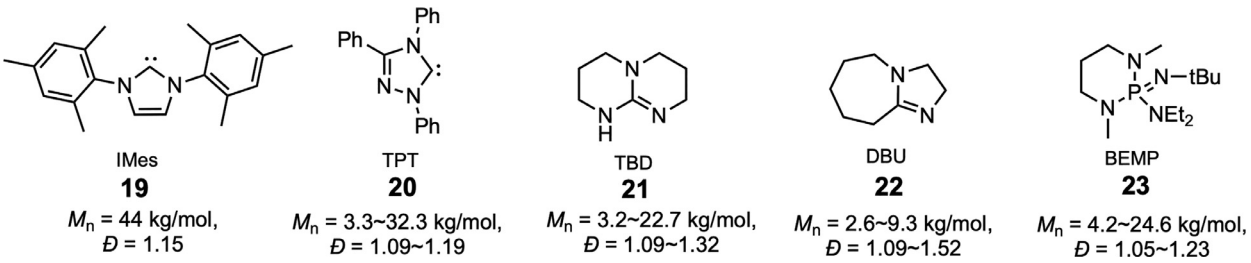

Fig. 7. Selected organocatalysts for non-stereoselective ROP of *rac*-β-BL to *at*-P3HB.

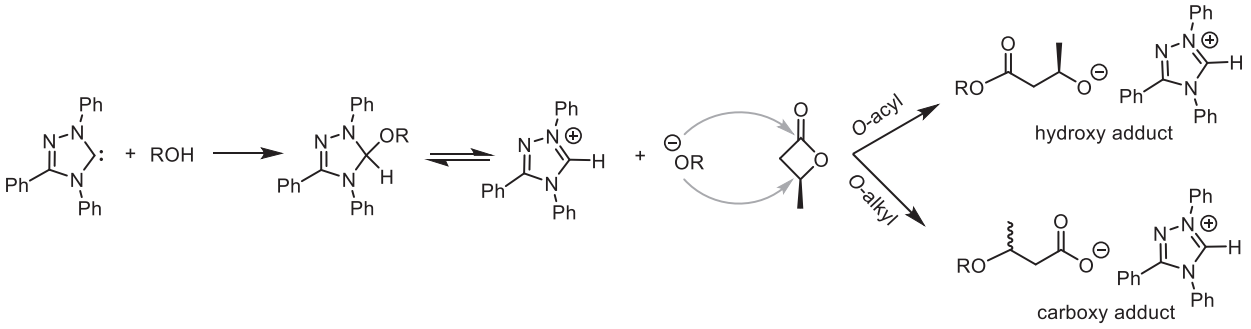

Scheme 6. Proposed mechanism of carbene initiation of *rac*-β-BL where the carboxy anion stabilized by the protonated carbene initiates ROP of *rac*-β-BL.

rac-β-BL that generate crotonate initiators [97]. To circumvent this issue, *tert*-butyl alcohol was added as cosolvent to favor adduct formation and minimize the concentration of the free carbene. Such conditions allowed for the controlled formation of *at*-P3HB although, when higher monomer loadings (>200 equiv.) were used to achieve higher molecular weights, the control was apparently lost. Mechanistic investigations revealed that the β-BL-carboxy anion, paired with the protonated carbene, was the initiating species (Scheme 6) [98]. Using *tert*-butyl alcohol in combination with TPT for the ROP of *rac*-β-BL brought about a living process absent of the crotonation side reaction, affording higher molecular weight polymer (32 kg/mol) with narrow $Đ$ values. This living process allowed for the synthesis of BCPs by the ROP of *rac*-β-BL initiated from poly(ethylene glycol)-α-methoxy,ω-carboxylic acid [98].

In comparison, TBD (1,5,7-triazabicyclo[4.4.0]dec-5-ene; **21**, Fig. 7), *N*-methyl-TBD, and DBU (1,8-diazabicyclo[5.4.0]-undec-7-ene; **22**, Fig. 7) were found to promote uncontrolled ROP of *rac*-β-BL [99]. This behavior was ascribed to a 1:1 adduct formation between β-BL and the guanidine/amidine organocatalyst, promoted by a strong hydrogen bonding of the hydroxy proton of the ring-opened β-BL to the adjacent nitrogen atom of the catalyst (Scheme 7). This 8-membered ring competes for hydrogen bond formation of the incoming alcohol of the initiator. Attempts to disrupt this adduct formation by increasing the temperature of the reaction resulted in the formation of oligomers with crotonate end-groups, highlighting the uncontrolled nature of the polymerization [99]. Jaffredo *et al.* overcame this problem with these basic organocatalysts by using specific reaction conditions and found that a reaction temperature of 60°C was crucial for enabling the controlled polymerization [100]. TBD had good control over molecular weight and dispersity, but BEMP, 2-*tert*-butylimino-2-diethylamino-1,3-dimethylperhydro-1,3,2-diazaphosphorine (**23**, Fig. 7), performed better overall.

Two mechanisms were proposed in the above study (Scheme 7). The first was the formation of the guanidine-β-BL adduct, followed by relatively fast dehydration to the corresponding *N*-acyl-α,β-unsaturated species, which then further propagates the chain via a living process (*Pathway 1*, Scheme 7). The alternative mechanism involves a zwitterion formed by partial dissociation of the organic base-β-BL adduct that ring-opens an incoming β-BL monomer (*Pathway 2*, Scheme 7). This second insertion is followed by propagation of the resulting zwitterion, and the crotonate end-groups would form via dehydration of the propagating species thus terminating the polymerization [100]. Moins *et al.* refuted this mechanism and instead contended that *rac*-β-BL is deprotonated by TBD, generating a crotonate anion stabilized by the large cation (the

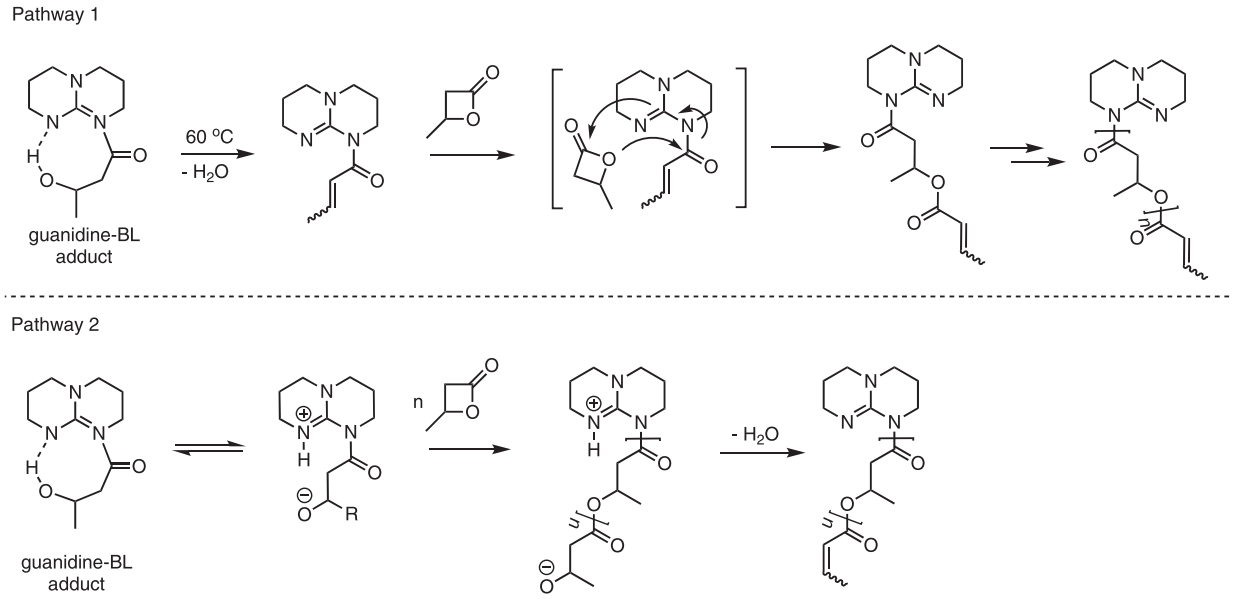

Scheme 7. Proposed two mechanistic pathways for the ROP of *rac*-β-BL by TBD.

protonated TBD), and this stabilized carboxylate acts as the initiating species [101]. In 2020, Shakaroun *et al.* reinvestigated this mechanism with alkoxymethylene-substituted β-BL [102], which will be discussed in Section 5 of this article. Nonetheless, the investigations above reveal that the mechanism operating in an organocatalyzed ROP of β-BL is highly dependent on the monomer substituent identity and the organocatalyst used, as well as the reaction conditions [100–102].

A series of bifunctional organoboron catalysts were used to efficiently polymerize *rac*-β-BL [103]. The authors proposed an initiation mechanism where *rac*-β-BL competitively coordinates to the boron center, allowing the dissociated anion to attack the activated β-BL either at the methine carbon to generate a benzoate active species or by abstracting an acidic proton thus proceeding via a crotonate active species. The end-group analysis provided evidence for the ROP to proceed via *O*-alkyl bond cleavage, generating a carboxylate-terminated P3HB.

4.2. Carbonylative polymerization of epoxides

The metal-catalyzed carbonylative ring-expansion reactions of heterocyclic compounds represent efficient one-step procedures to synthesize lactams, lactones, and thiolactones. Lee *et al.* observed that use of $Co_2(CO)_8$ and 3-hydroxypyridine (**27**, Fig. 8) as a cocatalyst for carbonylative ring-expansion of propylene oxide resulted in 75% polyester and only 15% β-BL formation [104]. On the other hand, ion pair $[PPN]^+[Co(CO)_4]^-$ (PPN = bis(triphenylphosphine)iminium, **24**, Fig. 8), in conjunction with a Lewis acid such as $BF_3{\bullet}Et_2O$, effectively catalyzed a range of regioselective carbonylation of aliphatic epoxides to afford β-lactones with yields ranging 57–87% [104].

Getzler *et al.* improved the yield of β-BL in carbonylation of epoxides by Lewis acids and oxyphilic cations capable of ether coordination [105]. Specifically, cationic aluminum salen-cobaltate complex, $[(salph)Al(THF)_2]^+[Co(CO)_4]^-$ (**25a**, Fig. 8) exhibited high activity (95% conversion of propylene oxide to β-BL in 1 h) with limited formation of polyester side products. The primary mechanistic pathway was proposed to undergo the nucleophilic attack of the activated epoxide at the less hindered site by anion $[Co(CO)_4]^-$ to give the β-lactone.

The above described carbonylative ring-expansion catalyzed by $Co_2(CO)_8$ and 3-hydroxypyridine (**27**, Fig. 8) afforded P3HB as the major product [104,106], which was reasoned through the direct alternating copolymerization of propylene oxide and CO, rather than by *in situ* ROP of the β-BL intermediate [106]. This mechanism was corroborated by three lines of evidence: 1) The rate of P3HB formation is independent of the presence of β-BL; 2) in fact, repeating the exact reaction conditions without the epoxide but with β-BL resulted in no P3HB formation, but the polymerization proceeded after addition of the epoxide to the reaction mixture; and 3) using the enantiopure epoxide resulted in exclusively *it*-P3HB even when *rac*-β-BL was present. More specifically, the mechanism was thought to be ring-opening of the epoxide and CO insertion at a tetracarbonyl cobaltate species. Pyridine appeared to be an essential part of the process, but its role was more obscure. Pyridine may assist in the electrophilic attack of the cobalt-bonded acyl carbon of the epoxide, and it may be involved in a back-biting reaction by deprotonating the –OH group to form β-BL as a side reaction [106]. In a subsequent study to better understand the mechanism of propagation and the chain termination events that shortened the resultant molecular weights, Allmendinger *et al.* observed retention of stereochemistry when using the enantiopure epoxide, thus supporting the mechanism previously suggested where CO inserts on the less sterically hindered side of the epoxide [107]. The major chain termination event observed was the hydrolysis of Co-acyl bonds and crotonic ester group formation via dehydration. There was also evidence for the direct coupling of two polymer chains which eliminated $Co_2(CO)_8$ and thus acting as another termination event.

While atom economy is preserved by the direct copolymerization of propylene oxide and CO, this method did not convert monomer at high rates, only produced low-molecular-weight polymers, and also resulted in the formation of β-BL as the side product. In an effort to increase the molecular weight, Lee and Alper changed 3-hydroxypyridine to the bulkier and more basic diamine, 6,7-dihydro-5,8-dimethyldibenzo[*b,j*]-1,10-phenanthroline and 2,9-dimethyl-4,7-diphenyl-1,10-phenanthroline which were used in conjunction with $Co_2(CO)_8$ and benzyl bromide in benzene (**28**, Fig. 8), P3HB was formed in higher molecular weight (M_n = 19 kg/mol) [108]. This method still achieved only a maximum of 55% P3HB yield after 20 h.

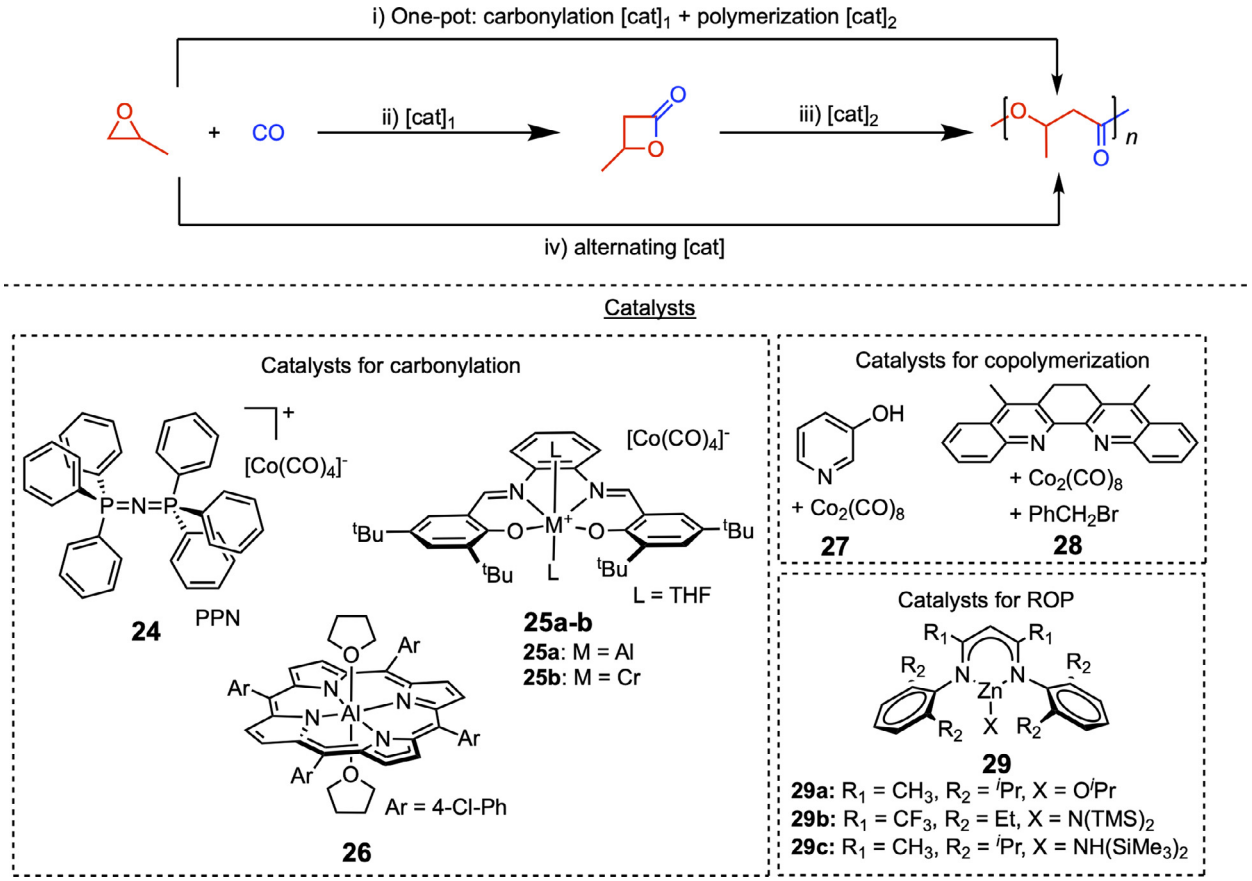

Fig. 8. Three routes to P3HB using carbonylation of epoxides with CO: (i) one-pot carbonylation and polymerization of the resulting β-BL by tandem catalytic transformations; (ii) first carbonylation of epoxide with CO, followed by (iii) ROP of the isolated β-BL; (iv) direct alternating copolymerization of propylene oxide epoxide and CO.

Dunn and Coates developed a one-pot tandem catalytic transformation where β-BL is synthesized from propylene oxide and CO by carbonylation catalysts and subsequently polymerized to *at*-P3HB with ROP catalysts *in situ* [109]. Multiple carbonylation catalysts were examined, but aluminum complex $[(ClTPP)Al(THF)_2]^+[Co(CO_4]^-$ (ClTPP = *meso*-tetra(4-chlorophenyl)porphyrinato) (**26**, Fig. 8) combined with the highly active zinc complex supported by bulky β-diiminate (BDI) ligands [(BDI)ZnO^{i}Pr; **29a**, Fig. 8] showed high activities for both carbonylation and ROP. Tuning the substituents on the Zn complex led to an optimized system, and higher molecular weight polymers (M_n up to 52 kg/mol) were produced. This process appeared to be living and, when the enantiopure epoxide was used, the tandem carbonylation/ROP process resulted in highly *it*-P3HB [109].

4.3. Metal-mediated coordinative-insertion ROP of rac-β-BL

As described in previous sections of this article, prior to the 2000s, most organometallic complexes studied for the ROP of β-BL were extremely slow or only resulted in low molecular weight P3HB. In 2002, Coates and co-workers employed discrete zinc alkoxy complex (BDI)ZnO^{i}Pr (**29a**, Fig. 8) to initiate the ROP of *rac*-β-BL and *rac*-β-valerolactone (β-VL) via a coordinative-insertion mechanism at unprecedented rates at that time to controlled, high molecular weight (M_n > 100 kg/mol), *at*-P3HB and poly(3-hydroxyvalerate) (P3HV), respectively [110].

A dimeric diaminophenolate zinc complex (**30**, Fig. 9) effectively polymerized up to 2000 equiv. of *rac*-β-BL in less than 30 min [111]. The resulting P3HB is syndio-enriched, but tuning the steric bulk on the ligand changed the syndiotacticity of the resulting polymer. For example, changing the *ortho* substituent from a cumyl (**30a**, Fig. 9) to adamantyl (**30b**, Fig. 9) increased the P_r value from 0.57 to 0.65 [111]. Immortal polymerization, where chain transfer is rapid and reversible thus forming polymers catalytically with narrow $Đ$ values [112], was achieved using the most syndioselective Zn complex, **30c** (Fig. 9) and up to 5,000 equiv. of benzyl alcohol as the effective chain transfer agent [111]. A Zn complex supported by the bulky bis(morpholinomethyl)phenoxy ligand (**31**, Fig. 9) is also effective for immortal polymerization of cyclic esters, converting 500 equiv. of *rac*-β-BL with 10 equiv. of ^{i}PrOH in 95% conversion within 3 h. The resulting *at*-P3HB had observed molecular weights similar to those calculated theoretically, indicating good control [113].

Another Zn(II) complex stabilized by a bidentate fluorous tertiary alkoxide-imino ligand (**32**, Fig. 9) promoted controlled ROP of *rac*-β-BL to *at*-P3HB [114]. This fluorous alkoxide ligand overcame the weakness of other alkoxide ligands which often produce highly aggregated polynuclear species due to the bridging tendency of the more basic alkoxide species compared to the phenoxide ligands. However, complex **32** (Fig. 9) showed a tendency to catalyze transesterification with prolonged reaction times, which resulted in broader dispersities and decreased molecular weights over time [114].

Group 4 (Ti, Zr, and Hf) complexes supported by 4,6-di-*tert*-butyl-2-phenylsulfanylphenol ligands (**33a-c**, Fig. 9) were also examined as catalysts for the ROP of *rac*-β-BL [113]. When combined with 5 equiv. of ^{i}PrOH, these complexes were moderately active and promoted "living" polymerization of *rac*-β-BL to *at*-P3HB [115]. Group 3 yttrium borohydride and alkoxide complexes supported by rigid dianionic bis(amide) ligands derived from 1,4-diaza-1,3-

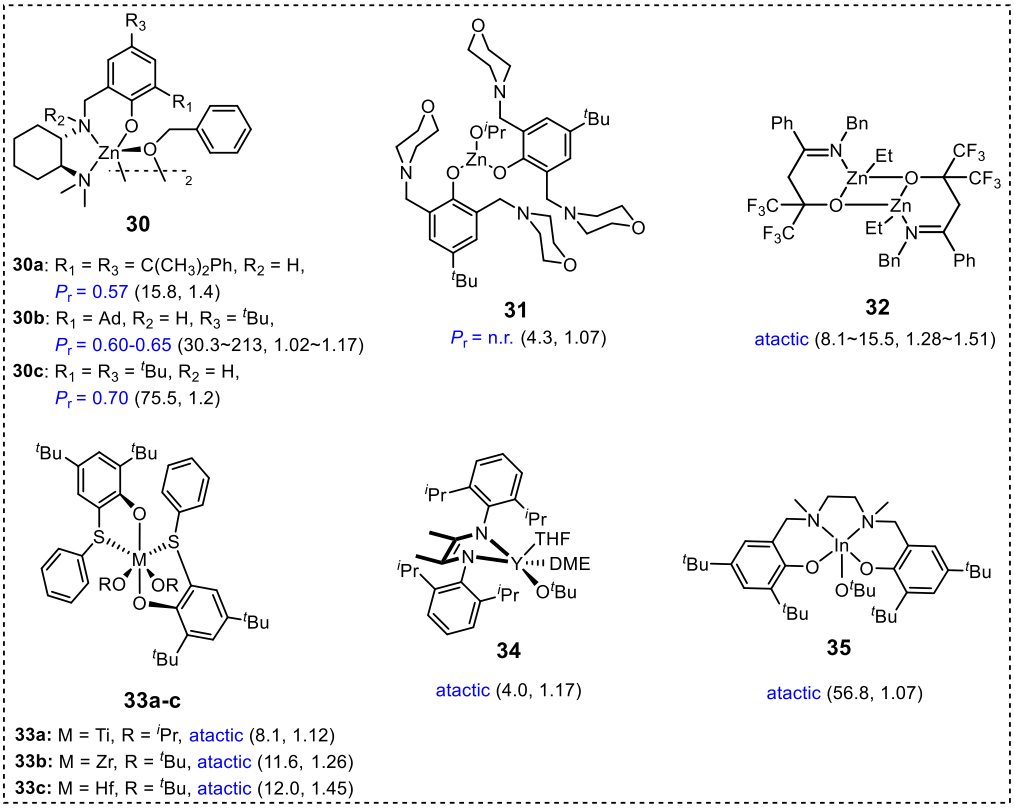

Fig. 9. Representative metal complexes for controlled, living, or immortal polymerization of *rac*-β-BL to largely *at*-P3HB. Dotted lines in 30 indicate a dimer. Ad = Adamantyl; n.r. = not reported, "atactic" = mention of the atactic microstructure based on ^{13}C NMR but no P_r values reported. M_n in kg/mol and $Đ$ values are placed in parentheses for each initiator.

butadiene (**34**, Fig. 9) were also investigated for their catalytic performance for the ROP of *rac*-β-BL to *at*-P3HB [116]. Generally, the ROP was very slow, but the observed molecular weights were in good agreement with the calculated values and the P3HB dispersities were narrow.

Salan-ligated indium complex **35** (Fig. 9) was found to have high activity and polymerization control, polymerizing 1000 equiv. of *rac*-β-BL in 8 h to P3HB with high M_n (56.8 kg/mol) and narrow dispersity ($Đ$ = 1.07) [117]. The polymerization proceeded under immortal conditions, allowing the use of up to 20 equiv. of chain transfer agent (benzyl alcohol) with no decrease in activity or control of the ROP.

5. Other PHA homopolymers and copolymers

5.1. Uncommon or unnatural PHAs

To understand the diversity of material properties of the PHA family and discover new PHA materials through PHA structure-property relationship studies, tuning the R pendant groups must be explored. One of the advantages of the chemocatalytic routes is the facile tuning of the monomer substituents that can lead to new PHAs, often uncommon or unnatural homopolymer PHAs and random or block copolymers.

Through the catalytic carbonylation of epoxides, which are often commercially available, a wide range of β-lactones, including β-lactones with fluorinated substituents were made available. The highly active (BDI)ZnO^{i}Pr (**29a**, Fig. 8) effectively polymerized such β-lactones into the resultant fluorinated PHAs (A, Fig. 10) [118]. In general, the fluorinated PHAs have higher T_g values than their non-fluorinated analogs. For example, naturally produced poly(β-hydroxyoctanoate) (P3HO) has a T_g of -35°C, while the fluorinated analog has a higher T_g of 4 °C. The direct carbonylative polymerization of a wide range of epoxides by a trimetallic (Cr) salen complex in combination with $Co_2(CO)_8$ led to generation of 17 new PHAs (M_n up to 38.2 kg/mol) with various structures, high regioselectivity (toward ring-opening of epoxides), diverse functionalities, and tunability as reflected in the wide ranging T_g values from as low as -45 °C to as high as 78 °C (B, Fig. 10) [119]. These examples further highlight the ability of the chemocatalytic route for facile tuning of the PHA structures.

Through stereoselective ROP of *rac*-8DL^R (R = Et, ^{n}Bu) by C_2-salen ligated yttrium complexes (11c and 11d), Chen *et al.* extended the chemocatalytic synthesis of PHAs to isotactic poly(3-hydroxyvalerate) (*it*-P3HV) and poly(3-hydroxyheptanoate) (*it*-P3HHp) (Scheme 8). These homopolymer PHAs are uncommon biologically, typically only found as random copolymers with *it*-P[(*R*)-P3HB]; thus, this simple chemical synthesis provides access to discrete homopolymer PHAs. It should be noted that P3HV and its copolymers can also be synthesized by the ROP of ethyl-substituted β-VL [110], but P3HHp is an uncommon PHA previously only accessible by highly engineered biological methods [120].

The stereoselective copolymerization of *rac*-8DL^{Me} with *rac*-8DL^R (R = Et, ^{n}Bu) yields high molecular weight (M_n >100 kg/mol, $Đ$ ~ 1.10), crystalline *it*-PHA copolymers (A, Fig. 11) [121]. As expected, increasing incorporation of *rac*-8DL^R decreases the crystallinity, T_m, and T_g of the resulting PHA copolymers. The mechanical properties of the random copolymers, poly(3-hydroxybutyrate-*co*-hydroxyvalerate) (P3HBV) and poly(3-hydroxybutyrate-*co*-hydroxyheptanoate) (P3HBHp) with ~7%, ~10%, and ~20% incorporation of *rac*-8DL^R, were analyzed via tensile testing of specimens prepared by compression molding (B and C, Fig. 11, and Table 1). P3HBV with 19.8% 3HV incorporation

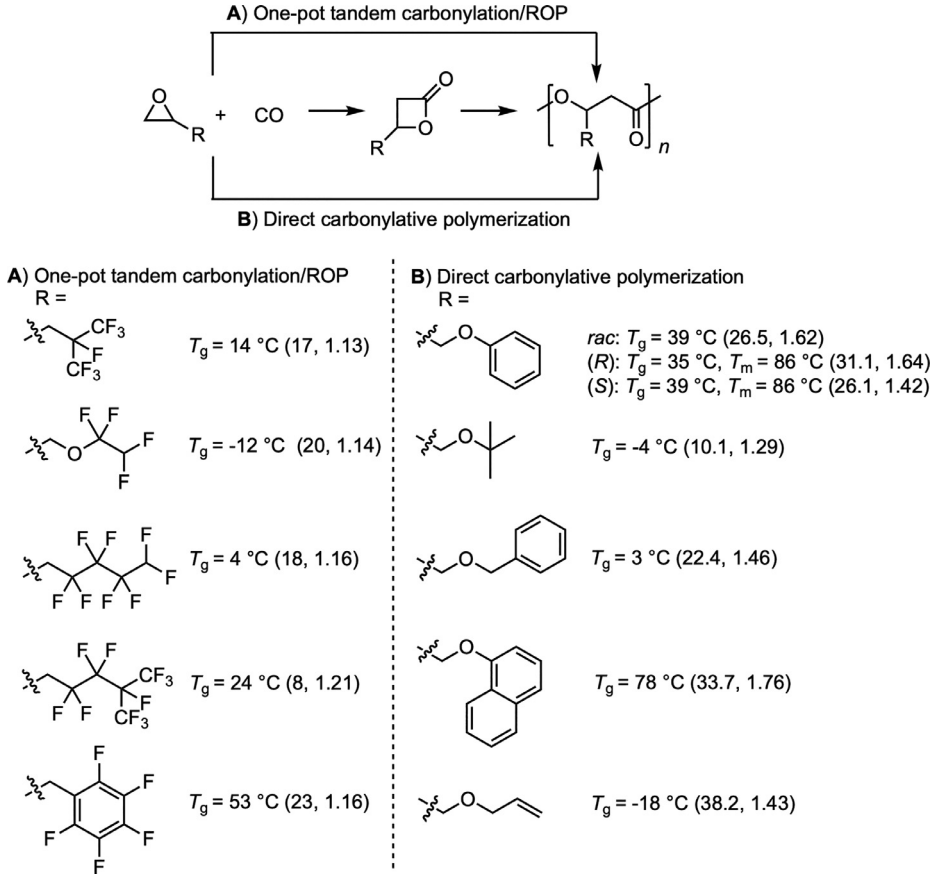

Fig. 10. (A) Tandem carbonylation/ROP and (B) direct carbonylative polymerization of epoxides for the synthesis of a wide range of fluoroalkyl-substituted and other alkyl- or oxo-alkyl (-CH_2-OR(Ar))-substituted PHAs. M_n in kg/mol and $Đ$ values are placed in parentheses for each initiator.

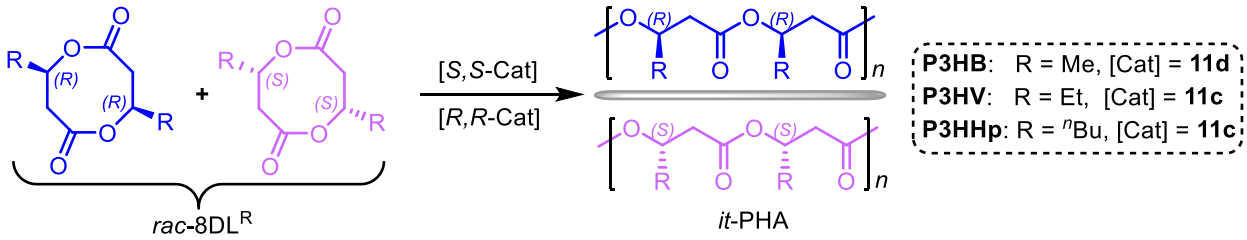

Scheme 8. Stereoselective ROP of *rac*-8DL^R to *it*-PHAs: R = Me, P3HB; R = Et, P3HV; R = ^{n}Bu, P3HHp.

showed polypropylene-like thermal and mechanical properties with σ = 25 ± 0.2 MPa, Young's Modulus (E) = 669 ± 45 MPa, and ε_B = 374 ± 19% (B, Fig. 11). On the other hand, the P3HBHp with 19.6% 3HHp incorporation exhibited polyethylene-like thermal and mechanical properties with σ = 20.5 ± 0.4 MPa, E = 226 ± 9 MPa, and ε_B = 578 ± 15% (C, Fig. 11). These results highlight the versatility and efficiency of the chemocatalytic synthesis via the stereoselective ROP of *rac*-8DL^R towards crystalline, *it*-PHA homopolymers and copolymers with tunable thermal and mechanical properties.

This catalyzed chemical synthesis was extended further to produce unnatural, aromatic PHAs with relatively high T_g and T_d (Fig. 12) [122]. Specifically, the ROP of benzyl substituted *meso*-8DL^{Bn} with Y and La complexes supported by C_2-Salen ligands affords syndiotactic ([*rr*] = 92%) poly(3-hydroxy-4-phenylbutyrate) (*st*-P3H4PhB) with high molecular weight (M_n = 147 kg/mol, $Đ$ = 1.19) and a high (relative to common PHAs) T_g of 43 °C (B, Fig. 12) [122]. Careful selection of catalyst, monomer, and conditions allowed for copolymerization of *meso*-8DL^{Bn} and *rac*-8DL^R (R = Me, ^{n}Bu) to produce aromatic-aliphatic random, stereotapered, or crystalline stereo-diblock PHA copolymers (A, Fig. 12). The statistical copolymerization of *meso*-8DL^{Bn} and *rac*-8DL^{Bu} gave high molecular weight (M_n = 205 kg/mol) copolymer, P3H4PhB-*co*-P3HHp, which is strong, hard, and ductile (ε_B = 191%) material, and displayed a high decomposition temperature, T_d = 281 °C (C, Fig. 12) (compared to ~250 °C for PHAs generally).

Li *et al.* reported a β-lactone fused with a five-membered ring at the α- and β-positions from the carbonylation of cyclopentene oxide with CO [123]. The coordinative-insertion ROP of this monomer using yttrium complex 10 with BnOH as initiator proceeds via *O*-acyl cleavage and produces a *cis*-PHA with a high T_m of ~ 185 °C (ΔH = 21 J/g) and a T_d of ~ 268 °C (Scheme 9). On the other hand, the organocatalyzed ROP with TBD (**21**) proceeds via *O*-alkyl cleavage and yields an amorphous, *trans*-PHA with a mixture of linear and cyclic topologies. Using yttrium complex **10** (Fig 4) alone (i.e., without an alcohol initiator) also produced a mixture of linear and cyclic topologies, and lanthanum complex **8** afforded the cyclic polymer as the major product. Ther-

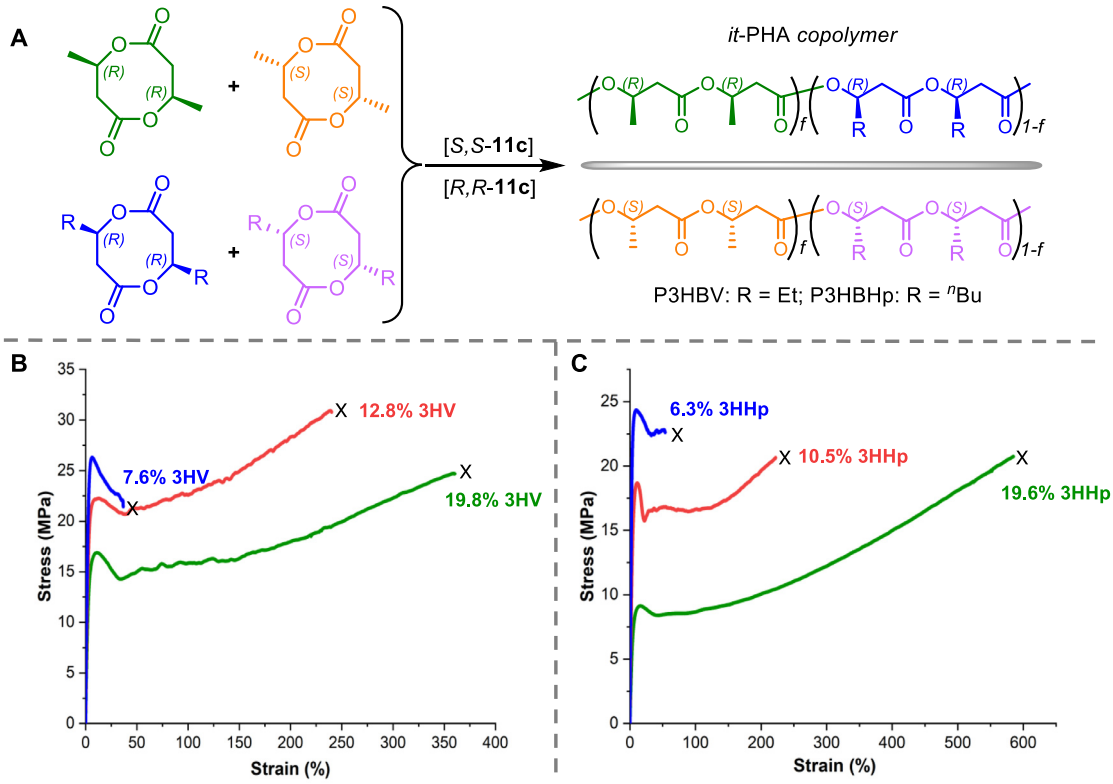

Fig. 11. (A) Stereoselective copolymerization of *rac*-8DL^{Me} with *rac*-8DL^{R} towards *it*-PHA copolymers. (B) Stress-strain overlay plots of P3HBV copolymers with varying 3HV incorporation. (C) Stress-strain overlay plots of P3HBHp copolymers with varying 3HHp incorporation.

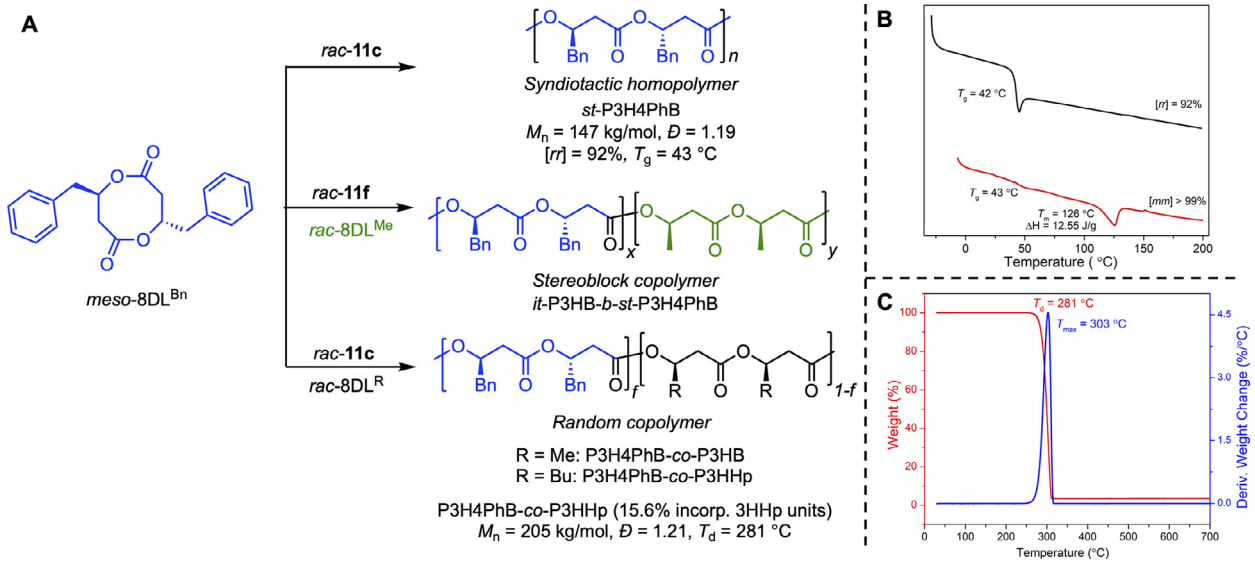

Fig. 12. (A) Aromatic PHAs from ROP of *meso*-8DL^{Bn}. B) DSC of *st*-P3H4PhB from ROP of *meso*-8DL^{Bn} (black) and *it*-P3H4PHB from ROP of *rac*-8DL^{Bn} (red, first heating scan). (C) TGA of P3H4PhB-*co*-P3HHp with 15.6% incorporation of 3HHp units [122]. Copyright 2020. Adapted with permission from American Chemical Society.

mal degradation (pyrolysis) of this α,β-cyclopentane fused PHA led to the formation of an α,β-unsaturated carboxylic acid, presenting a route for open-loop chemical recycling (Scheme 9) [123].

5.2. Functionalized or alternating PHAs

PHAs with functional groups can significantly modulate their physical, chemical, and mechanical properties, thereby becoming sought-after targets from chemocatalytic routes. The routes using functionalized β-BLs are commonly coupled with subsequent post-polymerization transformations of the resulting functionalized PHAs. For example, allyl-functionalized PHAs were synthesized by the ROP of *rac*-β-BL^{allyl} and its copolymerization with *rac*-β-BL using discrete amino-methoxy-bis(phenolate) yttrium-amido complex **9a** (Fig. 5) [77]. As expected, the ROP of *rac*-β-BL^{allyl} is slower than that of *rac*-β-BL, but the copolymers with various ratios of *rac*-β-BL and *rac*-β-BL^{allyl} are accessible by the controlled copolymerization that resulted in *st*-copolymer PHAs. Straightforward chemical transformations of the allyl pendant groups to respective alcohol, dihydroxyl, and epoxy derivatives were achieved

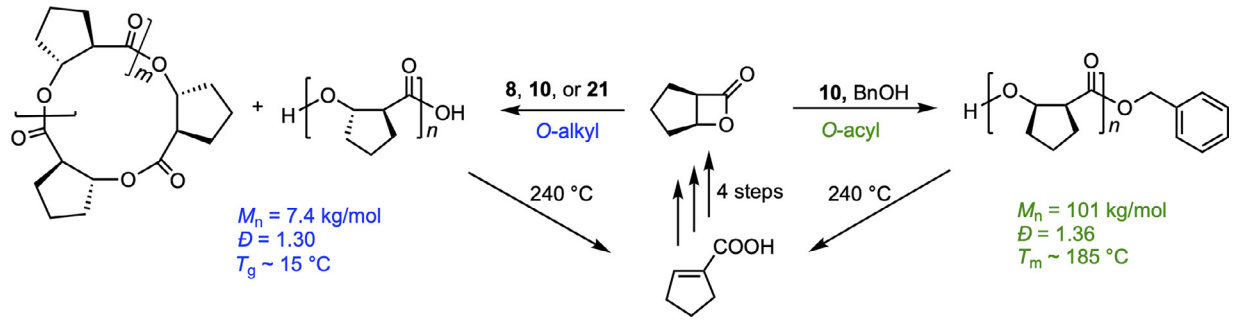

Scheme 9. ROP of α,β-substituted β-lactone to an α,β-cyclopentane-fused PHA with either linear or cyclic topology and its thermal degradation to cyclopentene carboxylic acid.

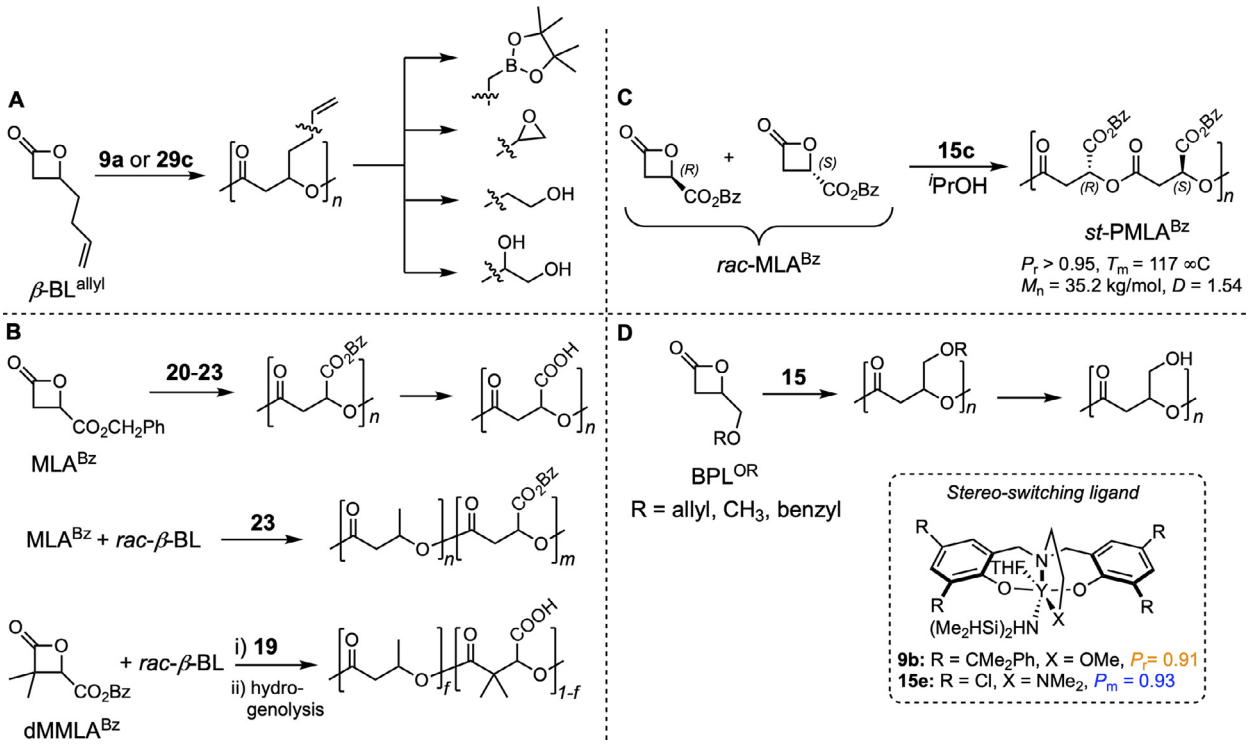

Scheme 10. ROP of functionalized β-BLs and chemical transformations of the resulting PHAs. (A) allyl-functionalized PHA and its post-polymerization functionalization into boron, epoxy, alcohol, and dihydroxyl PHA derivatives. (B) Carboxylic acid functionalized PHAs derived from benzyl-β-malolactone (MLA^{Bz}) and dimethyl benzyl β-malolactone (dMMLA^{Bz}). (C) Syndiotactic PMLA^{Bz} from stereoselective polymerization of *rac*-MLA^{Bz}. (D) Alkoxy functionalized β-propiolactone (*rac*-BPL^{OR}) and its stereoselective ROP en route to isotactic and syndiotactic PBPL^{OR} and the corresponding hydroxyl functionalized PHAs.

(A, Scheme 10), showcasing the tunability offered by the allyl-functionalized PHA.

Certain functional pendant groups such as protic (-OH and -COOH) groups cannot be introduced until after polymerization because of catalyst's functional group intolerance that can lead to suppression or inhibition of catalyst activity. Therefore, developing PHAs with pendant groups that can undergo post-polymerization modifications offers a promising route to accessing functional PHAs. With this strategy in mind, Guilaume *et al.* envisioned boron-containing PHAs for their use in the biomedical field, but attempts to polymerize a boron-functionalized *rac*-β-BL with Zn complex **29c** was unsuccessful, presumably due to catalyst inhibition by the polar boronate groups [124]. To solve this issue, the ROP of *rac*-β-BL^{allyl} with Zn complex 29c mixed *in situ* with BnOH, or Y complex 9a mixed *in situ* with ^{i}PrOH, was employed first to the allyl functionalized PHA, followed by hydroboration to afford the targeted boron-functionalized PHA (A, Scheme 10).

Through the ROP of benzyl-β-malolactone (MLA^{Bz}), followed by deprotection of *O*-benzyl groups via hydrogenolysis, hydrophilic PHAs carrying the carboxylic acid function have been developed (B, Scheme 10). The organocatalyzed ROP of MLA^{Bz} at 60°C with organic bases such as DBU and BEMP was efficient and controlled [125]. DBU and BEMP appeared to be more efficient than TBD for the ROP of MLA^{Bz}, and investigation into the mechanism revealed that the β-lactones are initiated by a 1:1 crotonate/TBD adduct or by a DBU/BEMP-*N*-acyl crotonate intermediate [125]. Simultaneous copolymerization of MLA^{Bz} with β-BL by BEMP led to di-BCP P(MLA^{Bz}-*b*-BL), due to drastic kinetic differences between MLA^{Bz} and β-BL (B, Scheme 10). On the other hand, the same copolymerization procedure by TBD and DBU resulted in only MLA^{Bz} conversion, thus yielding only the homopolymer (B, Scheme 10) [126]. Subsequently, a copolymerization procedure by sequential addition of MLA^{Bz} and β-BL afforded BCPs regardless of the order of addition for the above organic bases studied. These amphiphilic PMLA-*b*-P3HB copolymers as well as the BCPs from cyclic carbonates

and MLA^{Bz} were identified as biocompatible nanovectors for potential use for systemic drug delivery [127,128]. ROP of MLA^{Bz} by organometallic complex 15 results in highly syndiotactic polymer (C, Scheme 10) [129]

Poly([*R*/*S*]-3,3-dimethylmalic acid) (PdMMLA) is another attractive, water-soluble, aliphatic polyester with carboxylic pendant groups along the chain (B, Scheme 10), thanks to its biocompatibility and degradation to 3,3-dimethylmalic acid, a nontoxic molecule. The copolymerization of dimethyl benzyl β-malolactone (dMMLA^{Bz}) and *rac*-β-BL with triazole carbene **20** (Fig. 7) and ethylene glycol initiator proceeds via *O*-acyl cleavage of both dMMLA^{Bz} and β-BL with preferential incorporation of dMMLA^{Bz} but affords a random copolymer P(dMMLA^{Bz}-*co*-BL) (B, Scheme 10) [130]. Because of the diol initiation, the α,ω-dihydroxy P(dMMLA^{Bz}-*co*-BL) copolyester acts as a difunctional macroinitiator for L-lactide ROP to give an amphiphilic A-B-A tri-BCP after the *O*-benzyl groups were removed by hydrogenolysis.

PHAs with the hydroxyl function in the pendant group were produced by the ROP of *rac*-4-alkoxymethylene-β-propiolactone (*rac*-BPL^{OR}) derivatives, followed by chemical modifications of the resultant polymers with debenzylation, desilylation, or hydrogenolysis (D, Scheme 10) [131]. Contrary to the ROP of MLA^{Bz} by discrete yttrium complexes **15** where even small substituents on the *ortho* position of the phenoxy ligand can achieve high syndioselectivity [129], the ROP of *rac*-BPL^{OR} to highly syndiotactic polymer (P_r = 0.9) requires bulky *ortho* substituents on the phenolate ring [132]. Thus, the stereoselectivity was found to be strongly influenced by the nature of the *ortho* and *para* substituents on the phenolate ligand, due to steric and electronic secondary interactions between the ligand and monomer. In an intriguing twist, simply switching these *ortho* substituents from the bulky aromatic groups to halogens switches the stereochemical outcome from highly *st*- to *it*-polymer with P_m up to 0.93 (D, Scheme 10) [132]. For example, the cumyl substituted catalyst with an ether pendant arm (**9b**) resulted in highly *st*-PHB^{OR} with P_r = 0.91, but the chloride substituted catalyst with an amine pendant arm (**15c**) resulted in *it*-PHB^{OR} with P_m = 0.93 (D, Scheme 10) [131,132]. This stereoswitching strategy was extended to the ROP of *rac*-β-BL by yttrium complexes supported by a series of salan-like ligands with different R groups on the ligand framework of the bridging *N* atoms [133]. Aromatic phenyl groups on bridging *N* atoms afford isoenriched P3HB (P_m > 0.66). When the phenyl groups were replaced by aliphatic cyclohexyl groups, syndio-rich P3HB (P_r = 0.77) was obtained instead. Replacing this group with a *tert*-butyl group resulted in *at*-P3HB with P_m around 0.50 [133], providing another example showing that simple tuning of the ligand architecture can switch the stereoselectivity in the ROP of *rac*-β-BL.

Thomas, Coates, and co-workers developed a unique approach to access alternating syndiotactic PHA copolymers through copolymerization of a mixture of two enantiomerically pure, different β-lactones of opposite stereoconfiguration by a syndioselective yttrium-based catalyst (**36**, Scheme 11) [134]. These enantiopure β-lactones can be readily produced from carbonylation of the corresponding enantiopure epoxides, which were subject to copolymerization by the yttrium catalyst to produce various PHA copolymers with 90-94% alternation and T_m ranging from 47 to 210 °C, depending on the substituents (Me, Et, ^{n}Bu, $CH_2C_4F_9$, $CH_2OC_2H_5$) and their combinations.

This strategy has been extended to ROP of *rac*-BPL^{OR} using syndioselective catalyst **9b.** Alternating PHA copolymers, P(HB^{OR1}-*alt*-HB^{OR2}), can be conveniently synthesized via copolymerization of equimolar mixtures of (*R*)-BPL^{OR1} and (*S*)-BPL^{OR2} (A, Scheme 12) [135]. Changing to the isoselective Cl-substituted Y complex (**15c**) in combination with clever tuning of the monomer mixture can drastically change the resulting copolymer microstructures (B-C, Scheme 12). One such example is the polymerization of a 1:1 mixture of two differently substituted monomers of opposite stereoconfiguration, (*R*)-BPL^{OR1} + (*S*)-BPL^{OR2} into a mixture of two isotactic homopolymers, *it*-PHB^{OR1} + *it*-PHB^{OR2} (B, Scheme 12). On the other hand, when using differently substituted monomers of the same absolute configuration, (*S*)-BPL^{OR1} + (*S*)-BPL^{OR2}, *it*-(*S*)-chain random copolymer, (*S*)-P(BPL^{OR1}-*co*-BPL^{OR2}), was produced (C, Scheme 12). Lastly, using a racemic mixture of the differently substituted monomers, *rac*-BPL^{OR1} + *rac*-BPL^{OR2}, a mixture of *it*-(*S*)-chain random copolymers and *it*-(*R*)-chain random copolymers was produced (D, Scheme 12) [135].

As in the organocatalyzed ROP of *rac*-β-BL (*c.f.* Scheme 7), a recent investigation of the organocatalyzed ROP of BPL^{OR} using TBD, DBU, and BEMP to produce *at*-PHB^{OR} revealed that each organocatalyst carries a different mechanism of initiation [102]. Specifically, BEMP acts as a base and deprotonates the monomer to form the [carboxylate anion / protonated BEMP cation] ion pair which is the initiating species. Highly nucleophilic TBD forms a 1:1 *N*-acyl-α,β-unsaturated adduct via *O*-acyl cleavage of BPL^{OR} and this adduct propagates in a similar manner to BEMP. Lastly, DBU, which is both a nucleophile and base, favors scission of both *O*-acyl and *O*-alkyl bonds of BPL^{OR}, thus forming alkoxy and carboxylate active species.

5.3. Stereoblock or stereosequenced PHAs

A common practice for polymerizing a monomer bearing two stereogenic centers is to first separate its *racemic* and *meso* diastereomers and then subject the *rac*- or *meso*-diastereomer to different stereoselective catalysts to *it*- or *st*-polymer, respectively. In the case of 8DL^{Me}, the stereoselective ROP of *rac*-8DL^{Me} can produce perfectly *it*-polymer (P_m > 0.99) [72] while the stereoselective ROP of *meso*-8DL^{Me} can lead to highly *st*-polymer (P_r ~ 0.92) [93]. One might expect that the polymerization of the mixture of these diastereomers would result in a stereorandom, *at*-polymer. But in the diastereoselective polymerization system developed by Chen and co-workers, the racemic (*R,R*/*S,S*) yttrium and lanthanium complexes supported by C_2-symmetric salcy ligands with bulky, trityl *ortho* substituents (**11d**, Fig. 4 and **11f**, Scheme 5) were found to be both highly enantioselective [72] and diastereoselective, thus producing *it*/*st*-stereotapered diblock P3HB when directly polymerizing a *rac*/*meso*-8DL^{Me} mixture (Scheme 13) [93].

The diastereoselectivity that renders the formation of the tapered stereodiblock was revealed by monitoring of the polymerization of the 1:1 *rac*/*meso*-8DL^{Me} mixture, showing that *rac*-8DL^{Me} was rapidly polymerized within 30 s whereas *meso*-8DL^{Me} was much slower to react and required an additional 35 min to reach near quantitative conversion [93]. The monomer reactivity ratios of the copolymerization indicated a tendency for comonomers to form long, blocky segments. The isolated *it*-*sb*-*st*-P3HB was semicrystalline, having two T_c values of 87° and 69 °C and two corresponding T_m values of 135° and 115 °C associated with the respective *it*- and *st*-crystalline domains. Changing the *rac*/*meso*-8DL^{Me} ratio to 2:1 gave *it*-*sb*-*st*-P3HB with higher T_m values of 150° and 133 °C. The T_m values were further enhanced (by 6 to 10 °C) in the authentic stereodiblock P3HB synthesized by sequential addition of each diastereomer, due to the absence of the stereotapered junctions in this strereodiblock P3HB [93].

The *it*-*sb*-*st*-P3HB (50% *it*) showed enhanced ductility (ε_B = 17 ± 5%) compared to *it*-P3HB (ε_B < 5%), and the *it*-*sb*-*st*-P3HB (86% *it*) was similarly brittle to *it*-P3HB, thus highlighting the importance of the *st*-P3HB fraction in modulating mechanical properties. The ductility was drastically enhanced by copolymerizing 8DL^{Me} with 8DL^{Et} (*meso*-8DL^{Me} with *rac*-8DL^{Et}, as an example), which yielded a gradient stereo-BCP, *st*-P3HB-*sb*-*it*-P3HV (A, Fig. 13), due to the inherent diastereoselectivity between faster reacting *meso*-8DL^{Me} compared to *rac*-8DL^{Et} (B, Fig. 13). This stereo-BCP (18% 8DL^{Et} or 3HV incorporation) was shown to be a

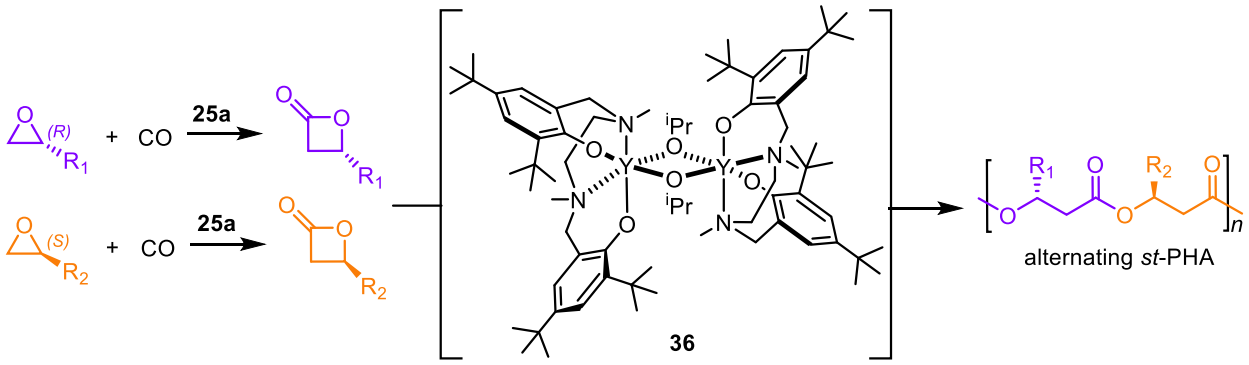

Scheme 11. Alternating *st*-PHA copolymers via syndioselective copolymerization of a pair of enantiopure β-lactones of opposite stereo-configuration.

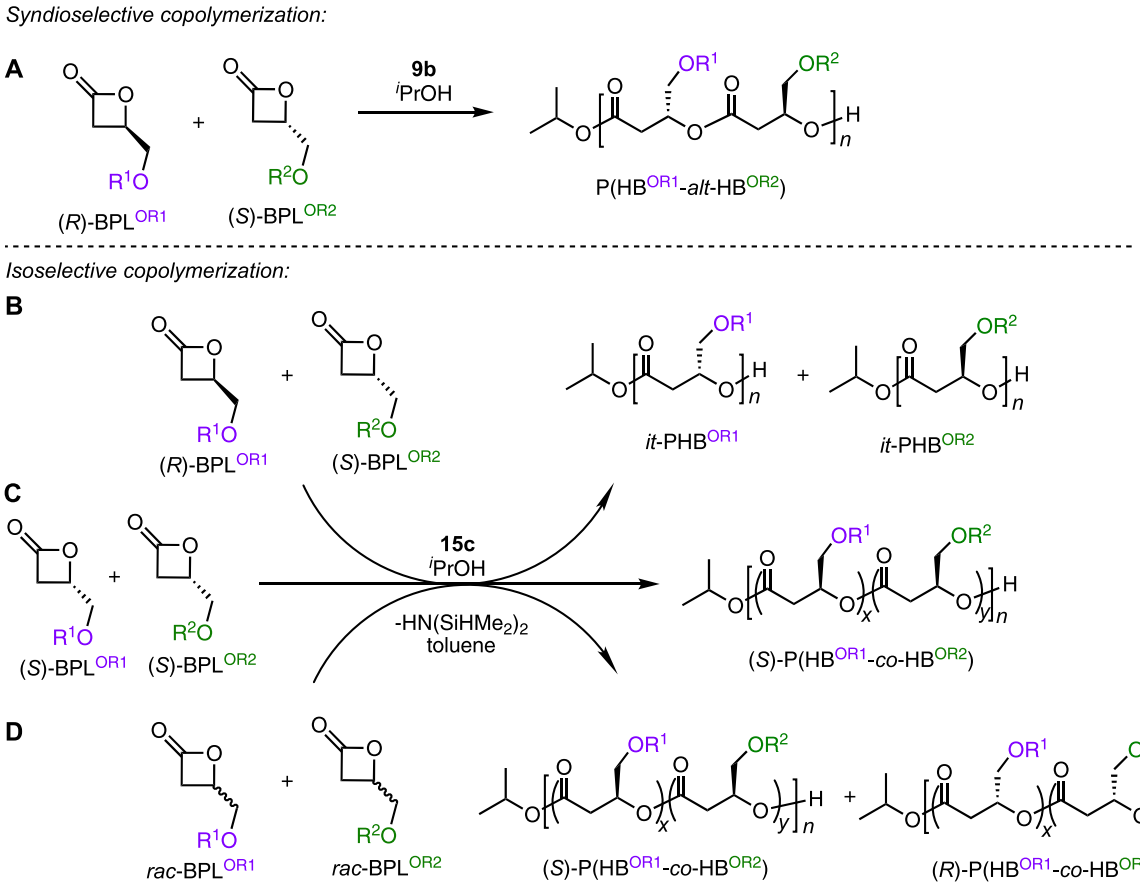

Scheme 12. A. Alternating copolymerization of different BPL comonomers of opposite stereo-configuration by syndioselective catalyst **9b**. B–D. Various homopolymer and copolymer compositions that can be achieved by copolymerizing mixtures of BPL^{OR1} + BPL^{OR2} with isoselective catalyst **15c**, depending on the configuration of paring comonomers.

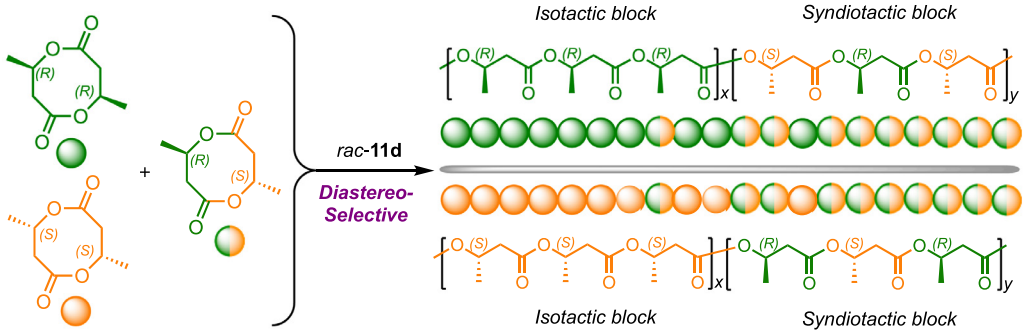

Scheme 13. Schematic representation of diastereoselective polymerization of the *rac/meso*-$8DL^{Me}$ mixture to *it/st*-stereotapered diblock, crystalline P3HB, *it-sb-st*-P3HB.

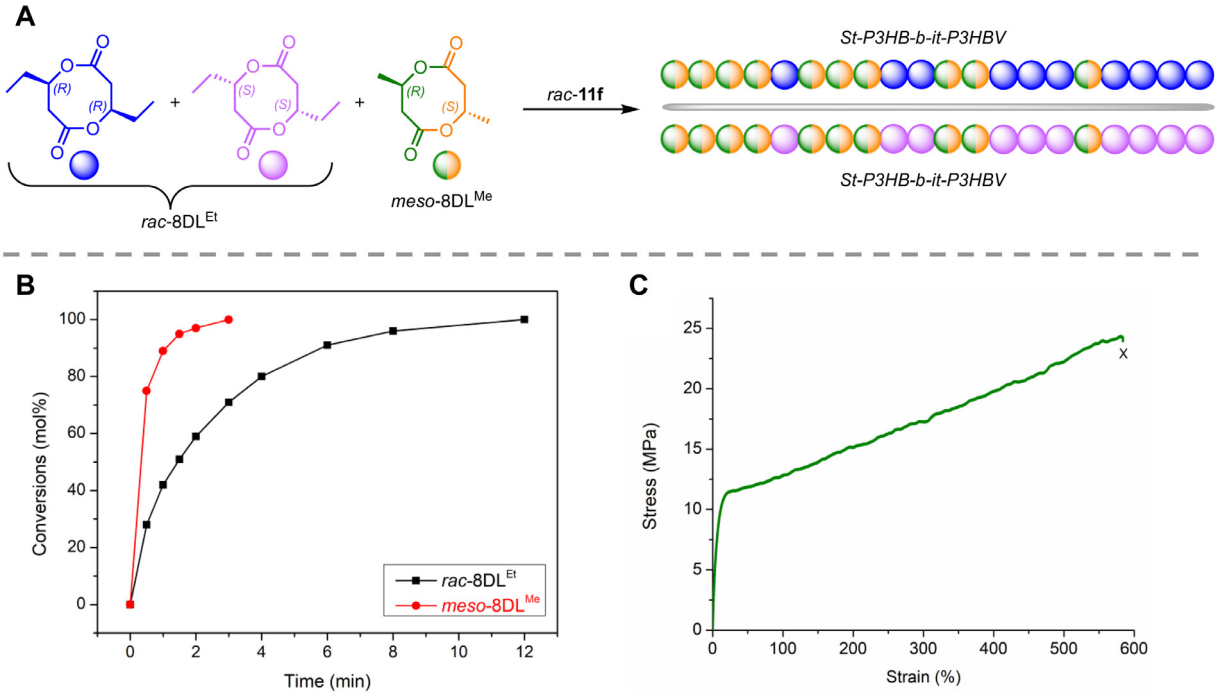

Fig. 13. A. Stereoblock copolymerization of *rac*-8DL^{Et} and *meso*-8DL^{Me} to produce a gradient stereo-BCP, *st*-P3HB-*sb*-*it*-P3HV. B. Kinetic plot of simultaneous polymerization of *rac*-8DL^{Et} and *meso*-8DL^{Me}. C. Stress-strain curve of *st*-P3HB-*sb*-*it*-P3HV (M_n = 113 kDa, $Đ$ = 1.27, 18% 3HV incorporation) [93]. Copyright 2019. Adapted with permission from American Association for the Advancement of Science.

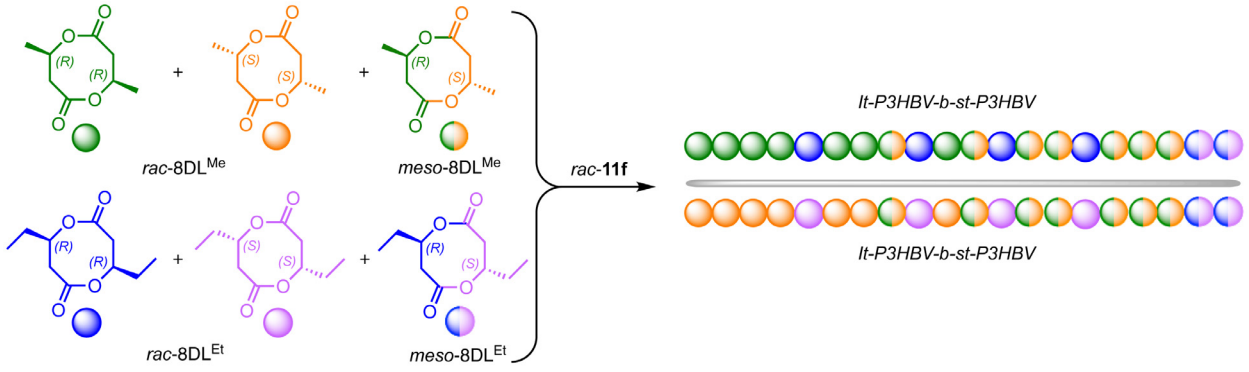

Scheme 14. Stereoblock copolymerization of diastereomeric mixtures of *rac*/*meso*-8DL^{Me} and *rac*/*meso*-8DL^{Et} to stereogradient di-BCP PHA.

strong, ductile, and tough material with relatively high ultimate strength (σ = 24.1 ± 1.5 MPa) and impressive elongation at break (ε_B = 564 ± 24%) (C, Fig. 13) [93].

Direct polymerization of all six 8DL$^{Me/Et}$ diastereomers together with a selective catalyst (*rac*-**11f**) yielded a stereogradient di-BCP consisting of the iso-rich P3HBV block and syndio-rich P3HBV block (Scheme 14) [93]. This sequencing was attributed to the established reactivity where *rac*-8DL^{Me} > *rac*-8DL^{Et}, *meso*-8DL^{Me} > *meso*-8DL^{Et}, and the catalyst's enantioselectivity toward the *rac* monomers and diastereoselectivity toward the *rac*/*meso* diastereomers. This stereogradient di-BCP is a semicrystalline material with a narrow $Đ$ value of 1.07. The scope was extended further to the synthesis of semicrystalline BCP *it*-P3HBHp-*sb*-*st*-P3HBHp, through copolymerization of a 1/1/1/1 diastereomeric mixture of *rac*/*meso*-8DL^{Bu} and *rac*/*meso*-8DL^{Me}. Overall, the unique catalyst-site-controlled diastereoselective methodology enables direct polymerization of diastereomeric mixtures of the same or different 8DL^{R} monomers (R = Me, Et, ^{n}Bu) into stereosequenced crystalline PHAs with tunable properties.

5.4. PHAs copolymers with other polyesters or polycarbonates

Copolymers of P3HB with other polymer segments or units through copolymerizations should substantially tailor the PHA properties by incorporating complementary comonomer units. A summary table comparing the thermal and mechanical properties of common polyolefins (*it*-PP, HDPE, LDPE), commercially available biodegradable plastics (PBAT and PBS), and several known "designer" PHAs are included at the end of this section (Table 1). Several examples of copolymerizing *rac*-β-BL with other lactones have been mentioned previously in this article [56,87,98]. Copolymers of lactide and β-BL have been studied and show interesting materials properties [55,136,137]. Tri-BCPs of *rac*-β-BL and both D- and L- lactides showed improved ε_B and some elastomeric behavior [138]. One particularly interesting copolymer of P3HB is from the terpolymerization of mixed monomer feedstocks consisting of *rac*-β-BL, cyclohexene oxide (CHO), and CO_2 using (BDI^{CF3})Zn[N(SiMe$_3$)$_2$] (**29b**, Fig. 8) [139]. This Zn complex catalyzes the alternating copolymerization of CHO and CO_2 to make

Table 1
Thermal and mechanical properties of PHA homopolymers and copolymers

Polymer	M_n (kDa)	T_g (°C)	T_m (°C)	E (MPa)	σ (MPa)	ε (%)	Reference
it-PP	97	~5	~160	1360	35	429	[a]
HDPE	7.6 (MFI)	~ -20	~130	1680	22	424	[a]
LDPE	7.5 (MFI)	~ -28	~110	190	12	385	[a]
PBAT	27.3	-30	110	126	16	560	[144]
PBS	116	~ -10	113	368	33	51	[144]
P3HB (P_m = 1.0) (bacteria)	n.r.	1	180	2500	36	3	[145]
P3HV (P_m = 0.97)	31.8	-17.5	108	587	9.6	2.3	[93]
P3HHp (P_m = 0.97)	126	-29.6	–	n.r.	n.r.	n.r.	[121]
it-P3HBV-*b*-*st*-P3HB (18% 3HV)	113	1.7	135	169	24.1	564	[93]
P3HBV (7.6% 3HV)	175	2.1	143	1166	25.8	35	[b]
P3HBV (12.8% 3HV)	138	0	136	856	31	257	[b]
P3HBV (19.8% 3HV)	119	-2.2	132	669	25.0	374	[121]
P3HBHp (6.3% 3HHp)	169	0	143	1056	25	58	[b]
P3HBHp (10.5% 3HHp)	183	-1.3	133	532	20.8	215	[b]
P3HBHp (19.6% 3HHp)	144	-7.6	127	226	20.5	578	[121]
P3HPhBHp (15.6% 3HHp)	205	33	–	1360	22.7	191	[122]
P3HB-*co*-PCHC (75/25 ratio)	101	n.r.	n.r.	150	5	350	[140]
P3HB-*b*-PCL (48.7% PCL)	70.6	3.3	54.4, 166	1450	20.5	106	[141]

[a] Because of the different values reported in literature, the mechanical properties (tensile modulus, *E*; ultimate stress, σ; elongation at break, ε) of these three polyolefin controls were measured in house using known processing conditions: *it*-PP, Sigma-Aldrich, film thickness = 0.83 ± 0.02 mm, hot-pressed at 190 °C, 30 min, 7 kpsi, slow cooling (>1 h); HDPE (melt-flow index, MFI = 7.6),), Goodfellow, film thickness = 0.783 ± 0.02 mm, hot-pressed at 150 °C, 30 min, 7 kpsi, slow cooling (>2 h); LDPE (MFI = 7.5), INEOS Olefins & Polymers Europe, film thickness = ~ 0.87 mm, hot-pressed at 125 °C, slow cooling (>2 h).

[b] The synthesis and mechanical properties of copolymers of varying composition were measured in house. All films were 0.80–0.84 mm thick, hot-pressed at 150 °C, 5 min, 5 kpsi, slow cooling (>1 h).

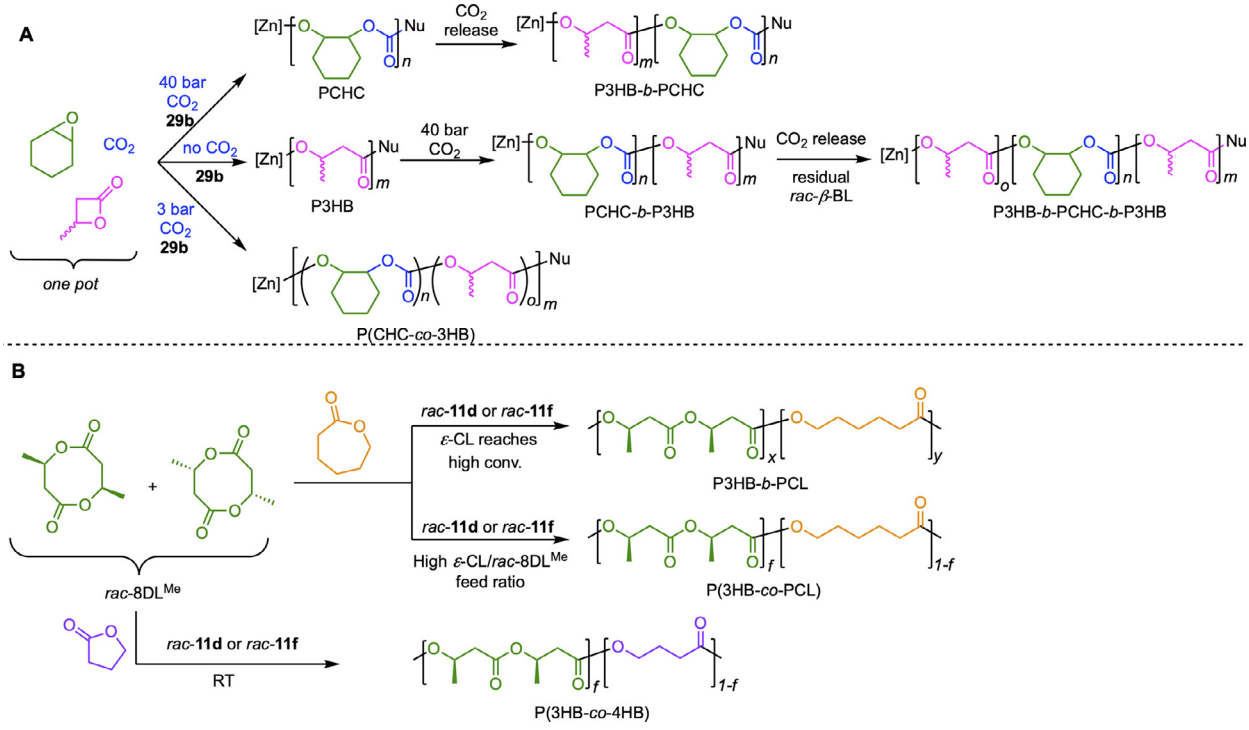

Scheme 15. Copolymers with other polyesters or polycarbonates. A. One-pot terpolymerization of CHO (green), *rac*-β-BL (pink), and CO_2 (blue) at varying CO_2 pressures to produce random or block copolymers. B. Copolymerization of *rac*-8DL^{Me} with ε-CL (orange) to block or random copolymers and with γ-BL (purple) to a random copolymer.

poly(cyclohexene carbonate) (PCHC), and the presence of CO_2 effectively turns off the ROP of *rac*-β-BL. This inhibition is attributed to CO_2 insertion into the Zn-O bond, leading to a carbonate chain end that is unable to ring-open an incoming *rac*-β-BL monomer. Thus, once CO_2 is released, the ROP of *rac*-β-BL begins again. Leveraging this on/off switch, tri-BCPs were synthesized by a one-pot method simply by increasing CO_2 pressure when *rac*-β-BL conversion reached 50% to produce P3HB-*b*-PCHC (A, Scheme 15). The CO_2 pressure was then released so that *rac*-β-BL continued polymerizing to full conversion to give the tri-BCP, P3HB-*b*-PCHC-*b*-P3HB. Low CO_2 pressure resulted in similar rates of both CHO/CO_2 copolymerization and ROP of *rac*-β-BL, thus forming statistical copolymers (A, Scheme 15) [139]. This work was later extended to show tunability of thermal and mechanical properties. For example, incorporation of some *at*-P3HB units into PCHC greatly enhanced the ε_B value from 1 to 350% [140].

Copolymerization of *rac*-8DL^{Me} with ε-caprolactone (ε-CL) and γ-butyrolactone (γ-BL) combines the desirable high crystallinity,

high T_m, and low gas permeability of P3HB with the high ductility of poly(ε-caprolactone) (PCL) and poly(γ-butyrolactone) (P4HB), thus making tougher biodegradable materials. In this context, a one-pot copolymerization of *rac*-8DL^{Me} and ε-CL comonomer mixture resulted in a di-BCP P3HB-*b*-PCL, thanks to the substantially higher rate of polymerization of *rac*-8DL^{Me} than that of ε-CL (the estimated initial k_p,*rac*-8DL^{Me}/ k_p,ε-CL is 28.8) (B, Scheme 15) [141]. By simply changing the conditions and comonomer feed ratio (using the ε-CL/*rac*-8DL^{Me} feed ratio $\geq$ 5/1 and quenching the reaction before *rac*-8DL^{Me} reaches full conversion to prevent formation of the long PCL block), semicrystalline random copolymers, P(3HB-*co*-CL) and P(3HB-*co*-4HB), can also be formed (B, Scheme 15). Mechanical testing of the BCP P3HB-*b*-PCL showed a strong and tough material with σ_B of 20.5 MPa, E of 1.45 GPa, and ε_B of 106%. Copolymerization of ε-decalactone and *rac*-β-BL using an yttrium bis(phenolate) catalyst (**36**, Scheme 11) led to the synthesis of BCPs PDL-*b*-*st*-P3HB (PDL = poly(ε-decalactone); P_r up to 0.90) and PDL-*b*-*st*-P3HB-*b*-PDL [142]. These copolymers were shown not to obey the Flory-Fox relationship as the microphase separation influences the T_g of both blocks [142].

Tri-BCPs of *st*-P3HB (P_r = 0.73) and poly((-)-menthide) (PM) were synthesized using a difunctional initiator and syndio-selective yttrium-bis(phenolate) catalyst (**9a**, Fig. 4) [143]. A copolymer of PM/*st*-P3HB = 45/56% (T_m = 110 °C) was compared to *st*-P3HB (P_r = 0.74, T_m = 117 °C) and the copolymer's E was drastically reduced (195 MPa vs 4.2 MPa) while the ε_B was increased (18 vs 35%) [143].

6. Conclusions and outlook

PHAs, thanks to their biodegradability in either managed or unmanaged environments and high structural tunability, are attracting ever increasing attention because they hold great potential to offer a practical solution to address the plastics pollution crisis and ever-growing needs for more sustainable materials that our society will rely on. However, the current high production costs and undesired performance properties of the PHAs produced by the biological routes largely limit their broader applications as commodity plastics. These challenges prompted the development of the chemocatalytic routes that can offer precision in synthesis—enabled by the living or controlled chain-growth ROP mechanism, greater tunability in polymer stereomicrostructures and the structures of monomers and molecular catalysts, as well as scalability and speed in polymer production. Advances to-date in the catalyzed chemical synthesis of PHAs have offered rapid access to highly *it*- and *st*-P3HB through the stereoselective ROP of β-BL and 8DL^{Me} enabled by the highly tunable chiral and achiral metal-based complexes that promote, often living or controlled, coordinative-insertion ROP. Rationally designed catalyst and monomer structures and insights obtained from mechanistic investigations have realized the precision synthesis of a wide range of PHAs, including PHA homopolymers of diverse stereomicrostructures as well as random, block and stereosequenced PHA copolymers that are often uniquely functionalized and uncommon or unnatural and inaccessible by biological methods. Some of the advanced, synthetic PHA materials offer thermal and mechanical properties that rival those of commodity polyolefins. Organic catalysts such as NHCs and superbases have offered new avenues towards the synthesis of *at*-PHAs that target sensitive applications in microelectronics and biomedical devices. As synthetic routes produce P3HB materials with diverse stereomicrostructures, it is important to examine their biodegradability or other types of degradation. In this context, racemic P3HB with P_m ranging from 0.63 to 0.92 has been found to completely biodegrade in 28 days and the rate of biodegradation is faster than for more crystalline, perfectly *it*-P3HB ([P(*R*)-3HB]) [146,147]. *St*-P3HB (P_r = 0.70) showed low biodegradation, but a blended film of *st*-P3HB (P_r = 0.70) and [P(*R*)-3HB] (P_m = 1.0) biodegraded completely [147].

Despite tremendous advances made in the chemocatalytic routes to PHAs over the past five decades, four key challenges are yet to be addressed:

First, concerning the cyclic ester monomers used for the two major routes, β-BL is toxic (possibly carcinogenic to humans), while 8DL^{R} monomers are currently prepared from a four-step synthesis starting from succinic acid but require the use of an alkyl halide and an oxidant, calling for more cost-effective and environmentally benign monomer synthesis. Addressing the monomer challenge would require efforts from multiple fronts, including the developments of greener synthetic routes, more benign monomer structures, selective recovery of monomers from PHAs (closed-loop chemical recycling, *vide infra*), and combined biocatalytic and chemocatalytic processes.

Second, the closed-loop chemical recycling of PHAs to their monomers is presently not realized. Base-catalyzed depolymerization of P3HB with catalysts such as $Mg(OH)_2$ afforded the dehydration product, *trans*-crotonic acid, in essentially quantitative yield (>97%) [148], but not the original lactone monomer (β-BL or 8DL^{Me}), while the acid-catalyzed depolymerization of P3HB with catalysts such as *p*-toluenesulfonic acid led to the formation of cyclic oligomers, with the major product being the highly stable, cyclic trimer (~50% yield) [149]. The ROP of this cyclic trimer reformed only oligomeric 3-hydroxybutyrate with low molecular weights (~5 kg/mol) [150,151], which cannot be considered a feasible route for closed-loop chemical recycling. Hence, there is a pressing need to develop an efficient, "monomer-polymer-monomer" closed-loop chemical recycling of PHAs, ultimately establishing the PHA-based circular materials economy. We believe that endowing polymers with chemical recyclability is important, especially in applications where plastic waste can be effectively collected and sorted. Even in the case of plastic mixtures, chemical recycling has also been shown to be feasible and advantageous due to the ability to selectively recover the monomer from the mixtures. These efforts, in conjunction with research and development in decreasing the complexity of final plastic products, will allow us to reach the ultimate goal of establishing carbon circularity.

Third, PHAs suffer from low thermostability towards melt-processing, particularly P3HB, with T_d values typically around 250 °C. This thermal property appears to be inherent to those unsubstituted PHAs at the 2 (or β)-position.

Fourth, the current synthetic PHAs are limited to offering properties of thermoplastics and elastomers. Endowing PHAs to deliver performance properties of other polymer classes, such as thermoplastic elastomers, reprocessable thermosets, and adhesives, will further broaden utilities of PHA-based materials and thus represents an exciting direction.

By way of critical analysis, the development of a biocatalytic route to the monomers for the ROP of the chemocatalytic route to PHAs should provide a desirable solution to meet the above stated first challenge of the chemocatalytic route. On the other hand, the second, third, and fourth challenges face both biocatalytic and chemocatalytic routes. Meeting those challenges will require innovative design of new monomers and catalyst structures, as well as the development of novel selective, greener, and catalytic processes for the synthesis of monomers and polymers, and their recovery and recycling. Future catalyst developments should be directed at enhancing selectivity/activity (thus lower catalyst loadings), enable recovery/recyclability (thus better economics), and utilizing more earth abundant metal or organic catalysts (thus more sustainable). Therefore, ultimately, the above challenges should be solved more effectively by coupling biocatalytic and chemocatalytic routes—the use of this preferred, synergistic catalysis mode to address the

plastics problems [152], including the above described challenges still facing PHAs.

Declaration of Competing Interest

The authors declare no competing interest.

Data Availability

No data was used for the research described in the article.

Acknowledgements

The work was supported in part by the US National Science Foundation (NSF-1955482) and by the U.S. Department of Energy, Office of Energy Efficiency and Renewable Energy (EERE), Advanced Manufacturing Office (AMO) and Bioenergy Technologies Office (BETO), as part of the BOTTLE™ Consortium, which includes the members from Colorado State University, under contract no. DE-AC36-08GO28308 with the National Renewable Energy Laboratory.

References

[1] Sudesh K, Abe H, Doi Y. Synthesis, structure and properties of polyhydroxyalkanoates: biological polyesters. Prog Polym Sci 2000;25:1503–55.
[2] Müller HM, Seebach D. Poly(hydroxyalkanoates): A fifth class of physiologically important organic biopolymers? Angew Chem Int Ed 1993;32:477–502.
[3] Lenz RW, Marchessault RH. Bacterial polyesters: biosynthesis, biodegradable plastics and biotechnology. Biomacromolecules 2005;6:1–8.
[4] Li Z, Yang J, Loh XJ. Polyhydroxyalkanoates: opening doors for a sustainable future. NPG Asia Mater 2016;8:e265 -20.
[5] Muhammadi S, Afzal M, Hameed S. Bacterial polyhydroxyalkanoates-eco-friendly next generation plastic: production, biocompatibility, biodegradation, physical properties and applications. Green Chem Lett Rev 2015;8:56–77.
[6] Chen GQ. A microbial polyhydroxyalkanoates (PHA) based bio- and materials industry. Chem Soc Rev 2009;38:2434–46.
[7] Taguchi S, Iwata T, Abe H, Doi Y. Poly(hydroxyalkanoate)s. In: Matyjaszewski K, Möller M, editors. Polymer science: a comprehensive reference, 9. Elsevier B. V.; 2012. p. 157–82.
[8] Narancic T, Verstichel S, Reddy Chaganti S, Morales-Gamez L, Kenny ST, De Wilde B, et al. Biodegradable plastic blends create new possibilities for end-of-life management of plastics but they are not a panacea for plastic pollution. Environ Sci Technol 2018;52:10441–52.
[9] Dilkes-Hoffman LS, Lant PA, Laycock B, Pratt S. The rate of biodegradation of PHA bioplastics in the marine environment: a meta-study. Mar Pollut Bull 2019;142:15–24.
[10] Meereboer KW, Misra M, Mohanty AK. Review of recent advances in the biodegradability of polyhydroxyalkanoate (PHA) bioplastics and their composites. Green Chem 2020;22:5519–58.
[11] Suzuki M, Tachibana Y, Kasuya K. Biodegradability of poly(3-hydroxyalkanoate) and poly(ε-caprolactone) via biological carbon cycles in marine environments. Polym J 2021;53:47–66.
[12] Laycock B, Halley P, Pratt S, Werker A, Lant P. The chemomechanical properties of microbial polyhydroxyalkanoates. Prog Polym Sci 2013;38:536–83.
[13] Sangroniz A, Zhu JB, Tang X, Etxeberria A, Chen EYX, Sardon H. Packaging materials with desired mechanical and barrier properties and full chemical recyclability. Nat Commun 2019;10:3559.
[14] Li M, Wilkins MR. Recent advances in polyhydroxyalkanoate production: feedstocks, strains and process developments. Int J Biol Macromol 2020;156:691–703.
[15] Amadu AA, Qiu S, Ge S, Addico GND, Ameka GK, Yu Z, et al. A review of biopolymer (Poly-β-hydroxybutyrate) synthesis in microbes cultivated on wastewater. Sci Total Environ 2021;756:143729.
[16] Chen GQ, Patel MK. Plastics derived from biological sources: Present and future: A technical and environmental review. Chem Rev 2012;112:2082–99.
[17] Madison LL, Huisman GW. Metabolic engineering of poly(3-hydroxyalkanoates): from DNA to plastic. Microbiol Mol Biol Rev 1999;63:21–53.
[18] Tan D, Wang Y, Tong Y, Chen GQ. Grand challenges for industrializing polyhydroxyalkanoates (PHAs). Trends Biotechnol 2021;39:953–63.
[19] Zia KM, Noreen A, Zuber M, Tabasum S, Mujahid M. Recent developments and future prospects on bio-based polyesters derived from renewable resources: a review. Int J Biol Macromol 2016;82:1028–40.
[20] Anjum A, Zuber M, Zia KM, Noreen A, Anjum MN, Tabasum S. Microbial production of polyhydroxyalkanoates (PHAs) and its copolymers: a review of recent advancements. Int J Biol Macromol 2016;89:161–74.
[21] Suriyamongkol P, Weselake R, Narine S, Moloney M, Shah S. Biotechnological approaches for the production of polyhydroxyalkanoates in microorganisms and plants - a review. Biotechnol Adv 2007;25:148–75.
[22] Wang Y, Yin J, Chen GQ. Polyhydroxyalkanoates, challenges and opportunities. Curr Opin Biotechnol 2014;30:59–65.
[23] Kumar G, Ponnusamy VK, Bhosale RR, Shobana S, Yoon JJ, Bhatia SK, Banu JR, Kim SH. A review on the conversion of volatile fatty acids to polyhydroxyalkanoates using dark fermentative effluents from hydrogen production. Bioresour Technol 2019;287:121427.
[24] Adeleye AT, Odoh CK, Enudi OC, Banjoko OO, Osiboye OO, Toluwalope Odediran E, Louis H. Sustainable synthesis and applications of polyhydroxyalkanoates (PHAs) from biomass. Process Biochem 2020;96:174–93.
[25] Tan D, Yin J, Chen GQ. Production of polyhydroxyalkanoates. In: Pandey A, Negi S, Soccol CR, editors. Current Developments in Biotechnology and Bioengineering. Elsevier; 2017. p. 655–92.
[26] Chee J, Yoga SS, Lau NS, Ling SC, Abed RMM, Sudesh K. Bacterially produced polyhydroxyalkanoate (PHA): converting renewable resources into bioplastics. Curr Res Technol Educ Top Appl Microbiol Microb Biotechnol 2010:1395–404.
[27] Bedade DK, Edson CB, Gross RA. Emergent approaches to efficient and sustainable polyhydroxyalkanoate production. Molecules 2021;26:3463.
[28] Steinbüchel A. Perspectives for biotechnological production and utilization of biopolymers: metabolic engineering of polyhydroxyalkanoate biosynthesis pathways as a successful example. Macromol Biosci 2001;1:1–24.
[29] Pederson EN, McChalicher CWJ, Srienc F. Bacterial synthesis of PHA block copolymers. Biomacromolecules 2006;7:1904–11.
[30] Li S, Cai L, Wu L, Zeng G, Chen J, Wu Q, et al. Microbial synthesis of functional homo-, random, and block polyhydroxyalkanoates by β-oxidation deleted Pseudomonas entomophila. Biomacromolecules 2014;15:2310–19.
[31] Ovitt TM, Coates GW. Stereoselective ring-opening polymerization of meso -lactide : synthesis of syndiotactic poly (lactic acid). J Am Chem Soc 1999;121:4072–3.
[32] Coates GW, Waymouth RM. Oscillating sterocontrol : a strategy for the synthesis of thermoplastic elastomeric polypropylene. Science 1995;267:217–19.
[33] Natta G. Properties of Isotactic, atactic, and stereoblock homopolymers, random and block copolymers of α-olefins. J Polym Sci 1959;34:531–49.
[34] Farina M. The stereochemistry of linear macromolecules. In: Eliel EL, Wilen SH, editors. Topics in stereochemistry. John Wiley & Sons, Inc.; 1987. p. 1–111.
[35] Hoskins JN, Grayson SM. Cyclic polyesters: synthetic approaches and potential applications. Polym Chem 2011;2:289–99.
[36] Steinbüchel A, Valentin HE. Diversity of bacterial polyhydroxyalkanoic acids. FEMS Microbiol Lett 1995;128:219–28.
[37] Seebach D, Bürger HM, Müller HM, Lengweiler UD, Beck AK. Synthesis of linear oligomers of (*R*) -3-hydroxybutyrate and solid-state structural investigations by electron microscopy and X-ray scattering. Helv Chim Acta 1994;77:1099–123.
[38] Kobayashi T, Hori Y, Kakimoto M, Imai Y. Synthesis of biodegradable polyesters by polycondensation of methyl (*R*)-3-hydroxybutyrate and methyl (*R*)-3-hydroxy- valerate. Makromol Chem Rapid Commun 1993;14:785–90.
[39] Lengweiler von UD, Fritz MG, Seebach D. Synthese monodisperser hearer und cyclischer oligomere der (*R*)-3-Hydroxybuttersaure mit bis zu 128 Einheiten. Helv Chim Acta 1996;79:670–701.
[40] Carpentier JF. Discrete metal catalysts for stereoselective ring-opening polymerization of chiral racemic β-lactones. Macromol Rapid Commun 2010;31:1696–705.
[41] Li H, Shakaroun RM, Guillaume SM, Carpentier JF. Recent advances in metal-mediated stereoselective ring-opening polymerization of functional cyclic esters towards well-defined poly (hydroxy acid)s: from stereoselectivity to sequence-control. Chem Eur J 2020;26:128–38.
[42] Carpentier JF. Rare-earth complexes supported by tripodal tetradentate bis(phenolate) ligands: a privileged class of catalysts for ring- opening polymerization of cyclic esters. Organometallics 2015;34:4175–89.
[43] Lecomte P, Jérôme C. Recent developments in ring-opening polymerization of lactones. In: Rieger B, Kunkel A, Coates GW, Reichardt R, Dinjus E, Zevaco TA, editors. Adv Polym Sci, 245. Elsevier; 2012. p. 173–217.
[44] Tang X, Chen EYX. Toward infinitely recyclable plastics derived from renewable cyclic esters. Chem 2019;5:284–312.
[45] Thomas CM. Stereocontrolled ring-opening polymerization of cyclic esters: Synthesis of new polyester microstructures. Chem Soc Rev 2010;39:165–73.
[46] Okada M. Chemical syntheses of biodegradable polymers. Prog Polym Sci 2002;27:87–133.
[47] Inoue S, Tomoi Y, Tsuruta T, Furukawa J. Organometallic-catalyzed polymerization of propiolactone. Makromol Chem. 1961;48:229–33.
[48] Zhang Y, Gross RA, Lenz RW. Stereochemistry of the ring-opening polymerization of (*S*)-β-butyrolactone. Macromolecules 1990;23:3206–12.
[49] Jedlinski Z, Kowalczuk M, Kurcok P, Matuszowicz A, Sikorska W, Gross RA, et al. Stereochemical control in the anionic polymerization of β-butyrolactone initiated with alkali-metal alkoxides. Macromolecules 1996;29:3773–7.
[50] Shelton JR, Agostini DE, Lando JB. Synthesis and characterization of poly-β-hydroxybutyrate. II. Synthesis of D-poly-β-hydroxybutyrate and the mechanism of ring-opening polymerization of β-butyrolactone. J Polym Sci Part A 1971;9:2789–99.
[51] Jedlinski Z, Kurcok P, Lenz RW. First facile synthesis of biomimetic poly-(*R*)-3-hydroxybutyrate via regioselective anionic polymerixation of (*S*)-β-butyrolactone. Macromolecules 1998;31:6718–20.
[52] Agostini DE, Lando JB, Shelton JR. Synthesis and characterization of poly-β-hydroxybutyrate. I. Synthesis of crystalline DL-Poly-β-hydroxybutyrate from DL-β-butyrolactone. J Polym Sci Part A 1971;9:2775–87.

[53] Tanahashi N, Doi Y. Thermal properties and stereoregularity of poly(3-hydroxybutyrate) prepared from optically active β-butyrolactone with a zinc-based catalyst. Macromolecules 1991;24:5732–3.

[54] Kemnitzer JE, Mccarthy SP, Gross RA. Poly (β-hydroxybutyrate) stereoisomers : a model study of the effects of stereochemical and morphological variables on polymer biological degradability. Macromolecules 1992;25:5927–34.

[55] Hori Y, Suzuki M, Yamaguchi A, Nishishita T. Ring-opening polymerization of optically active β-butyrolactone using distannoxane catalysts: synthesis of high molecular weight poly(3-hydroxybutryate). Macromolecules 1993;26:5533–4.

[56] Hori Y, Takahashi Y, Yamaguchi A, Nishishita T. Ring-opening copolymerization of optically active β-butryolactone with several lactones catalyzed by distannoxane complexes: synthesis of new biodegradable polyesters. Macromolecules 1993;26:4388–90.

[57] Tani H, Yamashita S, Teranishi K. Stereospecific polymerization of β-Methyl-β-propiolactone. Polym J 1972;3:417–18.

[58] Teranishi K, Iida M, Araki T, Yamashita S, Tani H. Stereospecific polymerization of β-alkyl-β-propiolactone. Macromolecules 1974;7:421–7.

[59] Iida M, Araki T, Teranishi K, Tani H. Effect of substituents on stereospecific polymerization of β-alkyl- and β-chloroalkyl-β-propiolactones. Macromolecules 1977;10:275–84.

[60] Bloembergen S, Holden DA, Bluhm TL, Hamer GK, Marchessault RH. Stereoregularity in synthetic β-hydroxybutyrate and β-hydroxyvalerate homopolyesters. Macromolecules 1989;22:1656–63.

[61] Yasuda T, Aida T, Inoue S. Living polymerization of β-butyrolactone catalysed by tetraphenylporphinatoaluminum chloride. Die Makromol Chem Rapid Commun 1982;3:585–8.

[62] Asano S, Aida T, Inoue S. Polymerization of Epoxide and β-lactone catalyzed by aluminum porphyrin. Exchange of alkoxide or carboxylate group as growing species on aluminum porphyrin. Macromolecules 1985;18:2057–61.

[63] Chen EYX, Marks TJ. Cocatalysts for metal-catalyzed olefin polymerization: activators, activation processes, and structure-activity relationships. Chem Rev 2000;100:1391–434.

[64] Wu B, Lenz RW. Stereoregular polymerization of [*R*,*S*]-3-butyrolactone catalyzed by alumoxane–monomer adducts. Macromolecules 1998;31:3473–7.

[65] Le Borgne A, Spassky N. Stereoelective polymerization of β-butyrolactone. Polymer 1989;30:2312–19 (Guildf).

[66] Zintl M, Molnar F, Urban T, Bernhart V, Preishuber-Pflügl P, Rieger B. Variably isotactic poly(hydroxybutyrate) from racemic β-butyrolactone: microstructure control by achiral chromium(III) salophen complexes. Angew Chem Int Ed 2008;47:3458–60.

[67] Reichardt R, Vagin S, Reithmeier R, Ott AK, Rieger B. Factors influencing the ring-opening polymerization of racemic β-butyrolactone using Cr III(salphen). Macromolecules 2010;43:9311–17.

[68] Vagin S, Winnacker M, Kronast A, Altenbuchner PT, Deglmann P, Sinkel C, et al. New insights into the ring-opening polymerization of β-butyrolactone catalyzed by chromium(III) salphen complexes. ChemCatChem 2015;7:3963–71.

[69] Dong X, Robinson JR. The role of neutral donor ligands in the isoselective ring-opening polymerization of *rac*-β-butyrolactone. Chem Sci 2020;11:8184–95.

[70] Dong X, Brown AM, Woodside AJ, Robinson JR. *N*-Oxides amplify catalyst reactivity and isoselectivity in the ring-opening polymerization of *rac*-β-butyrolactone. Chem Commun 2022;58:2854–7.

[71] Ajellal N, Durieux G, Delevoye L, Tricot G, Dujardin C, Thomas CM, et al. Polymerization of racemic β-butyrolactone using supported catalysts: a simple access to isotactic polymers. Chem Commun 2010;46:1032–4.

[72] Tang X, Chen EYX. Chemical synthesis of perfectly isotactic and high melting bacterial poly(3-hydroxybutyrate) from bio-sourced racemic cyclic diolide. Nat Commun 2018;9:2345.

[73] Hong M, Tang X, Newell BS, Chen EYX. "Nonstrained" γ-butyrolactone-based copolyesters: copolymerization characteristics and composition-dependent (thermal, eutectic, cocrystallization, and degradation) properties. Macromolecules 2017;50:8469–79.

[74] Tang X, Hong M, Falivene L, Caporaso L, Cavallo L, Chen EYX. The quest for converting biorenewable bifunctional α-methylene-γ-butyrolactone into degradable and recyclable polyester: controlling vinyl-addition/ring-opening/cross-linking pathways. J Am Chem Soc 2016;138:14326–37.

[75] Bouyahyi M, Ajellal N, Kirillov E, Thomas CM, Carpentier JF. Exploring electronic versus steric effects in stereoselective ring-opening polymerization of lactide and β-butyrolactone with amino-alkoxy-bis(phenolate)-yttrium complexes. Chem A Eur J 2011;17:1872–83.

[76] Amgoune A, Thomas CM, Ilinca S, Roisnel T, Carpentier JF. Highly active, productive, and syndiospecific yttrium initiators for the polymerization of racemic β-butyrolactone. Angew Chem Int Ed 2006;45:2782–4.

[77] Ajellal N, Bouyahyi M, Amgoune A, Thomas CM, Bondon A, Pillin I, et al. Syndiotactic-enriched poly(3-hydroxybutyrate)s via stereoselective ring-opening polymerization of racemic β-butyrolactone with discrete yttrium catalysts. Macromolecules 2009;42:987–93.

[78] Caputo MR, Tang X, Westlie AH, Sardon H, Chen EYX, Mu AJ. Effect of chain stereoconfiguration on poly (3-hydroxybutyrate) crystallization kinetics. Biomacromolecules 2022 Articles A.

[79] Kricheldorf HR, Berl M, Scharnagl N. Poly(lactones). 9. Polymerization mechanism of metal alkoxide initiated polymerizations of lactide and various lactones. Macromolecules 1988;21:286–93.

[80] Kricheldorf HR, Sumbél MV, Kreiser-Saunders I. Polylactones. 20. Polymerization of ε-caprolactone with tributyltin derivatives : a mechanistic study. Macromolecules 1991;24:1944–9.

[81] Kemnitzer JE, Mccarthy SP, Gross RA. Preparation of predominantly syndiotactic poly (β-hydroxybutyrate) by the tributyltin methoxide catalyzed ring-opening polymerization of racemic β-butyrolactone. Macromolecules 1993;26:1221–9.

[82] Kricheldorf HR, Lee S, Scharnagl N. Polylactones. 28. Syndiotactic poly(β-D,L-butyrolactone) by ring-opening polymerization of β-D,L-butyrolactone with butyltin methoxides. Macromolecules 1994;27:3139–46.

[83] Kemnitzer JE, Mccarthy SP, Gross RA. Syndiospecific ring-opening polymerization of β-butryolactone to form predominantly syndiotactic poly(β-hydroxybutryate) using tin(IV) catalysts. Mactromolecules 1993;26:6143–50.

[84] Kricheldorf HR, Polylactones LS. 35. Macrocyclic and stereoselective polymerization of β-D,L-butyrolactone with cyclic dibutyltin initiators. Macromolecules 1995;28:6718–25.

[85] Kricheldorf HR, Eggerstedt S. Polymerizations of β-D,L-butyrolactone with dialkyltinoxides as initiators. Macromolecules 1997;30:5693–7.

[86] Hori Y, Hagiwara T. Ring-opening polymerisation of β-butyrolactone catalysed by distannoxane complexes: study of the mechanism. Int J Biol Macromol 1999;25:237–45.

[87] Le Borgne A, Pluta C, Spassky N. Highly reactive yttrium alkoxide as new initiator for the polymerization of β-butyrolactone. Macromol Rapid Commun 1994;15:955–60.

[88] Cai CX, Toupet L, Lehmann CW, Carpentier JF. Synthesis, structure and reactivity of new yttrium bis(dimethylsilyl)amido and bis(trimethylsilyl)methyl complexes of a tetradentate bis(phenoxide) ligand. J Organomet Chem 2003;683:131–6.

[89] Nie K, Fang L, Yao Y, Zhang Y, Shen Q, Wang Y. Synthesis and characterization of amine-bridged bis(phenolate)lanthanide alkoxides and their application in the controlled polymerization of *rac*-lactide and *rac* -β -butyrolactone. Inorg Chem 2012;51:11133–43.

[90] Nie K, Feng T, Song F, Zhang Y, Sun H, Yuan D, et al. Bimetallic amine-bridged bis (phenolate) lanthanide aryloxides and alkoxides : synthesis, characterization, and application in the ring-opening polymerization of *rac*-lactide and *rac* -β-butyrolactone. Sci China Chem 2014;57:1106–16.

[91] Ajellal N, Lyubov DM, Sinenkov MA, Fukin GK, Cherkasov AV, Thomas CM, Carpentier JF, Trifonov AA. Bis(guanidinate) alkoxide complexes of lanthanides: synthesis, structures and use in immortal and stereoselective ring-opening polymerization of cyclic esters. Chem Eur J 2008;14:5440–8.

[92] Zeng T, Qian Q, Zhao B, Yuan D, Yao Y, Shen Q. Synthesis and characterization of rare-earth metal guanidinates stabilized by amine-bridged bis(phenolate) ligands and their application in the controlled polymerization of rac-lactide and rac-β-butyrolactone. RSC Adv 2015;5:53161–71.

[93] Tang X, Westlie AH, Watson EM, Chen EYX. Stereosequenced crystalline polyhydroxyalkanoates from diastereomeric monomer mixtures. Science 2019;366:754–8.

[94] Kamber NE, Jeong W, Waymouth RM, Pratt RC, Lohmeijer BGG, Hedrick JL. Organocatalytic ring-opening polymerization. Chem Rev 2007;107:5813–40.

[95] Kiesewetter MK, Shin EJ, Hedrick JL, Waymouth RM. Organocatalysis: opportunities and challenges for polymer synthesis. Macromolecules 2010;43:2093–107.

[96] Connor EF, Nyce GW, Myers M, Mock A, Hedrick JL. First example of N-heterocyclic carbenes as catalysts for living polymerization: organocatalytic ring-opening polymerization of cyclic esters. J Am Chem Soc 2002;124:914–15.

[97] Coulembier O, Lohmeijer BGG, Dove AP, Pratt RC, Mespouille L, Culkin DA, Benight SJ, Dubois P, Waymouth RM, Hedrick JL. Alcohol adducts of N-heterocyclic carbenes: latent catalysts for the thermally-controlled living polymerization of cyclic esters. Macromolecules 2006;39:5617–28.

[98] Coulembier O, Delva X, Hedrick JL, Waymouth RM, Dubois P. Synthesis of biomimetic poly(hydroxybutyrate): alkoxy- and carboxytriazolines as latent ionic initiator. Macromolecules 2007;40:8560–7.

[99] Lohmeijer BGG, Pratt RC, Leibfarth F, Logan JW, Long DA, Dove AP, Nederberg F, Choi J, Wade C, Waymouth RM, Hedrick JL. Guanidine and amidine organocatalysts for ring-opening polymerization of cyclic esters. Macromolecules 2006;39:8574–83.

[100] Jaffredo CG, Carpentier JF, Guillaume SM. Controlled ROP of β-butyrolactone simply mediated by amidine, guanidine, and phosphazene organocatalysts. Macromol Rapid Commun 2012;33:1938–44.

[101] Moins S, Henoumont C, Winter JD, Khalil A, Laurent S, Cammas-Marion S, et al. Reinvestigation of the mechanism of polymerization of β-butyrolactone from 1,5,7-triazabicyclo[4.4.0]dec-5-ene. Polym Chem 2018;9:1840–7.

[102] Shakaroun RM, Jehan P, Alaaeddine A, Carpentier JF, Guillaume SM. Organocatalyzed ring-opening polymerization (ROP) of functional β-lactones: new insights into the ROP mechanism and poly(hydroxyalkanoate)s (PHAs) macromolecular structure. Polym Chem 2020;11:2640.

[103] Yang L, Zhang YY, Yang GW, Xie R, Wu GP. Controlled ring-opening polymerization of β-butyrolactone via bifunctional organoboron catalysts. Macromolecules 2021;54:5509–17.

[104] Lee JT, Thomas PJ, Alper H. Synthesis of β-lactones by the regioselective, cobalt and lewis acid catalyzed carbonylation of simple and functionalized epoxides. J Org Chem 2001;66:5424–6.

[105] Getzler Y, Mahadevan V, Lobkovsky EB, Coates GW. Synthesis of β-lactones: a highly active and selective catalyst for epoxide carbonylation. J Am Chem Soc 2002;124:1174–5.
[106] Allmendinger M, Eberhardt R, Luinstra G, Rieger B. The cobalt-catalyzed alternating copolymerization of epoxides and carbon monoxide: a novel approach to polyesters. J Am Chem Soc 2002;124:5646–7.
[107] Allmendinger M, Eberhardt R, Luinstra GA, Rieger B. Alternating copolymerization reaction of propylene oxide and CO: variation of polymer stereoregularity and investigation into chain termination. Macromol Chem Phys 2003;204:564–9.
[108] Lee JT, Alper H. Alternating copolymerization of propylene oxide and carbon monoxide to form aliphatic polyesters. Macromolecules 2004;2:2417–21.
[109] Dunn EW, Coates GW. Carbonylative polymerization of propylene oxide: a multicatalytic approach to the synthesis of poly(3-hydroxybutyrate). J Am Chem Soc 2010;132:11412–13.
[110] Rieth LR, Moore DR, Lobkovsky EB, Coates GW. Single-site β-diiminate zinc catalysts for the ring-opening polymerization of β-butyrolactone and β-valerolactone to poly(3-hydroxyalkanoates). J Am Chem Soc 2002;124:15239–48.
[111] Ebrahimi T, Aluthge DC, Hatzikiriakos SG, Mehrkhodavandi P. Highly active chiral zinc catalysts for immortal polymerization of β-butyrolactone form melt processable syndio-rich poly(hydroxybutyrate). Macromolecules 2016;49:8812–24.
[112] Inoue S. Immortal polymerization: the outset, development, and application. J Polym Sci Part A Polym Chem 2000;38:2861–71.
[113] Poirier V, Roisnel T, Carpentier JF, Sarazin Y. Versatile catalytic systems based on complexes of zinc, magnesium and calcium supported by a bulky bis(morpholinomethyl)phenoxy ligand for the large-scale immortal ring-opening polymerisation of cyclic esters. Dalton Trans 2009:9820–7.
[114] Grunova E, Roisnel T, Carpentier JF. Zinc complexes of fluorous alkoxide-imino ligands: synthesis, structure, and use in ring-opening polymerization of lactide and β-butyrolactone. Dalton Trans 2009:9010–19.
[115] Luciano E, Buonerba A, Grassi A, Milione S, Capacchione C. Thioetherphenolate group 4 metal complexes in the ring opening polymerization of *rac*-β-butyrolactone. J Polym Sci Part A Polym Chem 2016;54:3132–9.
[116] Mahrova TV, Fukin GK, Cherkasov AV, Trifonov AA, Ajellal N, Carpentier JF. Yttrium complexes supported by linked bis(amide) ligand: synthesis, structure, and catalytic activity in the ring-opening polymerization of cyclic esters. Inorg Chem 2009;48:4258–66.
[117] Bruckmoser J, Henschel D, Vagin S, Rieger B. Combining high activity with broad monomer scope: indium salan catalysts in the ring-opening polymerization of various cyclic esters. Catal Sci Technol 2022;12:3295–302.
[118] Kramer JW, Coates GW. Fluorinated β-lactones and poly(β-hydroxyalkanoate)s: synthesis via epoxide carbonylation and ring-opening polymerization. Tetrahedron 2008;64:6973–8.
[119] Yang JC, Yang J, Li WB, Lu XB, Liu Y. Carbonylative polymerization of epoxides mediated by tri-metallic complexes: a dual catalysis strategy for synthesis of biodegradable polyhydroxyalkanoates. Angew Chem Int Ed 2022;61:e202116208.
[120] Wang H, Li X, Chen GQ. Production and characterization of homopolymer polyhydroxyheptanoate (P3HHp) by a fadBA knockout mutant Pseudomonas putida KTOY06 derived from P. putida KT2442. Process Biochem 2009;44:106–11.
[121] Tang X, Westlie AH, Caporaso L, Cavallo L, Falivene L, Chen EYX. Biodegradable polyhydroxyalkanoates by stereoselective copolymerization of racemic diolides: stereocontrol and polyolefin- like properties research articles. Angew Chem Int Ed 2020;59:2–12.
[122] Westlie AH, Chen EYX. Catalyzed chemical synthesis of unnatural aromatic polyhydroxyalkanoate and aromatic – aliphatic PHAs with record-high glass-transition and decomposition temperatures. Macromolecules 2020;53:9906–15.
[123] Li YT, Yu HY, Li WB, Liu Y, Lu XB. Recyclable polyhydroxyalkanoates via a regioselective ring-opening polymerization of α,β-disubstituted β-lactone monomers. Macromolecules 2021;54:4641–8.
[124] Guillaume C, Ajellal N, Carpentier JF, Guillaume SM. Boron–functionalized poly(3-hydroxybutyrate)s from hydroboration of poly(allyl-β-hydroxyalkanoate)s: synthesis and insights into the microstructure. J Polym Sci Part A Polym Chem 2010;49:907–17.
[125] Jaffredo CG, Carpentier JF, Guillaume SM. Organocatalyzed controlled ROP of β-lactones towards benzyl β-malolactone polymers. Polym Chem 2013;4:3837–50.
[126] Jaffredo CG, Carpentier JF, Guillaume SM. Poly(hydroxyalkanoate) block or random copolymers of β-butyrolactone and benzyl β-malolactone: a matter of catalytic tuning. Macromolecules 2013;46:6765–76.
[127] Barouti G, Jarnouen K, Cammas-Marion S, Loyer P, Guillaume SM. Polyhydroxyalkanoate-based amphiphilic diblock copolymers as original biocompatible nanovectors. Polym Chem 2015;6:5414–29.
[128] Barouti G, Khalil A, Orione C, Jarnouen K, Cammas- S, Loyer P, Guillaume SM. Poly(trimethylene carbonate)/poly(malic acid) amphiphilic diblock copolymers as biocompatible nanoparticles. Chem Eur J 2016;22:2819–30.
[129] Jaffredo CG, Chapurina Y, Kirillov E, Carpentier JF, Guillaume SM. Highly stereocontrolled ring-opening polymerization of racemic alkyl β-malolactonates mediated by yttrium [amino-alkoxy-bis(phenolate)] complexes. Chem Eur J 2016;22:7629–41.
[130] Coulembier O, Mespouille L, Hedrick JL, Waymouth RM, Dubois P. Metal-free catalyzed ring-opening polymerization of β-lactones: synthesis of amphiphilic triblock copolymers based on poly(dimethylmalic acid). Macromolecules 2006;39:4001–8.
[131] Ligny R, Hänninen MM, Guillaume SM, Carpentier JF. Highly syndiotactic or isotactic polyhydroxyalkanoates by ligand-controlled yttrium-catalyzed stereoselective ring-opening polymerization of functional racemic β-lactones. Angew Chem Int Ed 2017;56:10388–93.
[132] Ligny R, Hänninen MM, Guillaume SM, Carpentier JF. Steric vs. electronic stereocontrol in syndio- or iso-selective ROP of functional chiral β-lactones mediated by achiral yttrium-bisphenolate complexes. Chem Commun 2018;54:8024–31.
[133] Zhuo Z, Zhang C, Luo Y, Wang Y, Yao Y, Yuan D, et al. Stereo-selectivity switchable ROP of *rac*-β-butyrolactone initiated by salan-ligated rare-earth metal amide complexes: the key role of the substituents on ligand frameworks. Chem Commun 2018;54:11998–2001.
[134] Kramer JW, Treitler DS, Dunn EW, Castro PM, Roisnel T, Thomas CM, Coates GW. Polymerization of enantiopure monomers using syndiospecific catalysts : a new approach to sequence control in polymer synthesis. J Am Chem Soc 2009;131:16042–4.
[135] Ligny R, Guillaume SM, Carpentier JF. Yttrium-mediated ring-opening copolymerization of oppositely configurated 4-alkoxymethylene-β-propiolactones: effective access to highly alternated isotactic functional PHAs. Chem Eur J 2019;25:6412–24.
[136] Jeffery BJ, Whitelaw EL, Garcia-Vivo D, Stewart JA, Mahon MF, Davidson MG, et al. Group 4 initiators for the stereoselective ROP of *rac*-β-butyrolactone and its copolymerization with rac-lactide. Chem Commun 2011;47:12328–30.
[137] Reeve MS, Mccarthy SP, Gross RA. Preparation and characterization of (*R*)-poly(β-hydroxybutyrate)-poly(ε-caprolactone) and (*R*)-poly(β-hydroxybutyrate)-poly(lactide) degradable diblock copolymers. Macromolecules 1993;26:888–94.
[138] Aluthge DC, Xu C, Othman N, Noroozi N, Hatzikiriakos SG, Mehrkhodavandi P. PLA-PHB-PLA triblock copolymers: synthesis by sequential addition and investigation of mechanical and rheological properties. Macromolecules 2013;46:3965–74.
[139] Kernbichl S, Reiter M, Adams F, Vagin S, Rieger B. CO_2-controlled one-pot synthesis of AB, ABA block, and statistical terpolymers from β-butyrolactone, epoxides, and CO_2. J Am Chem Soc 2017;139:6787–90.
[140] Kernbichl S, Reiter M, Mock J, Rieger B. Terpolymerization of β-butyrolactone, epoxides, and CO_2: chemoselective CO_2-switch and its impact on kinetics and material properties. Macromolecules 2019;52:8476–83.
[141] Tang X, Shi C, Zhang Z, Chen EYX. Toughening biodegradable isotactic poly(3-hydroxybutyrate) via stereoselective copolymerization of a diolide and lactones. Macromolecules 2021;54:9401–9.
[142] Kiriratnikom J, Robert C, Guérineau V, Venditto V, Thomas CM. Stereoselective ring-opening (co)polymerization of β-butyrolactone and ε-decalactone using an yttrium bis(phenolate) catalytic system. Front Chem 2019;7.
[143] Adams F, Pehl TM, Kränzlein M, Kernbichl SA, Kang JJ, Papadakis CM, et al. (Co)polymerization of (-)-menthide and β-butyrolactone with yttrium-bis(phenolates): tuning material properties of sustainable polyesters. Polym Chem 2020;11:4426–37.
[144] Zhang Q, Song M, Xu Y, Wang W, Wang Z, Zhang L. Bio-based polyesters: recent progress and future prospects. Prog Polym Sci 2021;120:101430.
[145] Martin DP, Williams SF. Medical applications of poly-4-hydroxybutyrate: a strong flexible absorbable biomaterial. Biochem Eng J 2003;16:97–105.
[146] Abe H, Matsubara I, Doi Y, Hori Y, Yamaguchi A. Physical properties and enzymatic degradability of poly(3-hydroxybutyrate) stereoisomers with different stereoregularities. Macromolecules 1994;27:6018–25.
[147] Abe H, Doi Y. Enzymatic and environmental degradation of racemic poly(3-hydroxybutyric acid)s with different stereoregularities. Macromolecules 1996;29:8683–8.
[148] Ariffin H, Nishida H, Shirai Y, Hassan MA. Highly selective transformation of poly[(*R*)-3-hydroxybutyric acid] into trans-crotonic acid by catalytic thermal degradation. Polym Degrad Stab 2010;95:1375–81.
[149] Seebach D, Müller H, Bürger HM, Plattner DA. The triolide of (*R*)-3-hydroxybutyric acid – direct preparation from polyhydroxybutyrate and formation of a crown estercarbonyl complex with Na ions. Angew Chem Int Ed 1992;31:434–5.
[150] Melchiors M, Keul H, Höcker H. Synthesis of highly isotactic poly[(*R*)-3-hydroxybutyrate] by ring-opening polymerization of (*R,R,R*)-4,8,12-trimethyl-1,5,9-trioxacyclododeca-2,6,10-trione. Macromol Rapid Commun 1994;15:497–506.
[151] Melchiors M, Keul H, Höcker H. Depolymerization of poly[(R)-3-hydroxybutyrate] to cyclic oligomers and polymerization of the cyclic trimer: an example of thermodynamic recycling. Macromolecules 1996;29:6442–51.
[152] Ellis LD, Rorrer NA, Sullivan KP, Otto M, McGeehan JE, Román-Leshkov Y, Wierckx N, Beckham GT. Chemical and biological catalysis for plastics recycling and upcycling. Nat Catal 2021;4:539–56.